

SUBSOIL EVALUATION IN GEOMORPHOLOGICALLY UNSTABLE CONDITION USING GEOPHYSICAL AND GEOTECHNICAL METHODS AT OKE-IGBO, SOUTHWESTERN NIGERIA

¹*Afolabi Rasaq Kolawole ²Olayanju Gbenga Moses ³Ikubuwaje Christopher Olatunde ⁴Tanimola Moses Oladejo

^{1,2}Department of Applied Geophysics, Federal University of Technology, Akure Nigeria

³School of Engineering, Federal Polytechnic, Ado-Ekiti, Nigeria

⁴Department of Civil Engineering, Federal University of Technology, Akure Nigeria

¹rasakafolabi@gmail.com

²gmolayanju@futa.edu.ng

³cikubuwaje@gmail.com

⁴engrtanimola@gmail.com

Corresponding author E-mail: rasakafolabi@gmail.com

Abstract

The competency of the subsoil material for engineering site characterization in a Geomorphological unstable Oloruntele town a suburb of Oke Igbo was evaluated using geophysical and geotechnical methods in producing an integrity assessment of the subsurface geology. The deployed geophysical measurements involved running both electrical resistivity imaging with the aids of dipole-dipole array in conjunction with vertical electrical sounding along the established traverses, followed by geotechnical analyses. Specific geotechnical analyses conducted include the gravimetric, hydraulic conductivity and strength tests of the collected soil samples along road segment that traverse the study area. The results of the resistivity imaging revealed conductive zones and geologic features identified as fractures and cavities, which can affect the competency of the subsoil as sub-base or subgrade foundation materials. The zones were characterized by relatively low resistivity values; the cavities were observed to probably consist of materials moved into their present positions from materials from the landslide that occurred along the section of the study area, which aggravated creeping of the soil materials from the hilly terrain. From the electrical soundings conducted, four distinct geoelectric layers were delineated that comprise the topsoil, weathered layer, fractured bedrock and fresh bedrock. Furthermore, values in the range of 4-15%, 2.6-2.7 g/cm³, 1.6-28.7%, 19-33%, 21-22%, 4-11%, 1-7, 1.2×10^{-5} - 1.9×10^{-3} cm/s, 1810-1880 kg/m³, 4-6%, 31-79%, 219-312 KPa and 102-156 KPa were obtained from geotechnical parameters; viz soil natural moisture content, specific gravity, percentage of finer, Liquid limits, plastic limits, plasticity index, Linear shrinkage, permeability, Maximum dry

density, Optimum moisture content, California bearing ratio, Unconfined compression test and undrained shear strength respectively, resulting from the geotechnical analysis of the soil samples which indicates that the soil in the area are majorly sand and loose fragments of nearby quartzite ridge, which can easily move under gravity when heavy load are applied on them.

Keywords: Electrical resistivity method, Dipole-Dipole array, vertical electrical sounding, geotechnical competence, consistency test, grain-size, California bearing ratio, Hydraulic test.

1.0 INTRODUCTION

The origin of the increased failure in engineering structures such as roads, buildings, and bridges throughout the southwestern region of Nigeria has been a major problem. Some of the factors responsible for these failures had been linked to inadequate supervision, poor construction materials, non-compliance to standard specifications, among notable causes. Several studies have shown that these failures can also be attributed to lack of adequate information on the nature of subsurface conditions prior to construction since all engineering structures are believed to be seated on geological earth materials (Mesida, 1987; Ajayi, 1987; Momoh et al., 2008; Oladapo et al., 2008; Adiat et al., 2009., Adeyemo and Omosuyi, 2012).

Some major geologic factors comprising exact depth to bedrock and its lithological type, lateral changes in lithology, and detection of fractures, cracks, or faults are essential to designing formidable foundations and assessing the integrity of civil engineering structures (Olayanju *et al.*, 2017). Bedrock relief (or depression) can also precipitate instability (Adeyemo and Omosuyi, 2012). In addition, the nature of topsoil (subgrade) and the near surface geologic sequence, and existence of ancient stream channels and shear zones constitute geohazards that can impair stability of any road structure (Adiat et al., 2017). The need for site characterization must be given adequate consideration in order to prevent loss of valuable lives and properties that always accompany infrastructural failures. Road transportation has been an important element in the physical development of any society as it controls the direction and extent of development (Bolaji, 2003). Good roads devoid of failed sections to promote economic growth of a nation by creating enabling environment for the movement of goods and services. A good network of roads will facilitate such movement and hence enhance the economy of the nation. It will also reduce haulage vehicle accidents thereby minimizing human and material losses.

Civil engineers for reason of cost and other consideration sometimes do not include geophysical investigation of subsoil competency before carrying out road construction work. Cases where such

studies are done, the findings are not taken into consideration in the design and construction phase. The result of this omission is usually failed structures which can manifest as ground subsidence, major cracks, failed road segment and fractional settlement of the structure (Olorunfemi *et al.*, 2000; Olorunfemi *et al.*, 2004).

The art and practice of geophysics in the study of earth and its evolving processes has grown to a reliable means of undertaking shallow-depth investigations to assist in civil engineering works as related to the geologic nature, hydrogeology/drainage pattern and geomorphology of the environment.

The conditions of Nigerian roads for instance have been a lot of concern due to increasing infrastructural deplorable conditions that are making negative impacts on the socio-developmental state of the country at large. An agrarian community like this study area are under the siege of deplorable road conditions that are predicted to be linked with the geologic terrain arising from tectonic activities and or several environmental factors (Rahman, 1988; Folami, 1998).

In addition to the manmade activities, environmental impacts from geo-hazards such as landslides, slope failure, weathering and erosion due to heavy rainfall could also create shallow depressions or void that are filled with weak materials. Effects of these factors in some cases might not immediately manifest on the surface, hence the need to carry out subsoil investigation in order to know both the lateral and vertical variations of the geologic units in the area. It is in this regard that a section of road linking Oloruntele to major area of agricultural activities in geomorphological unstable parts of Oke-Igbo, southwestern Nigeria was embarked on to evaluate the competency of the subgrade soils in order to facilitate proper road construction plan for such deplorable environment.

2.0 THE STUDY AREA

The study area is underlain by basement complex terrain of the crystalline rocks of Nigeria (Rahaman and Malomo, 1983; Jegede, 1999). The major rock is mainly the medium grained granite gneisses, the medium grained granite gneisses are strongly foliated and commonly occurring as outcrops and quartzite which form ridges have undergone series of tectonic activities (Figure 1). These two rock-types are part of the complex lithology and tectonic framework of Ilesha belt in the southwestern Nigeria. Ilesha has been studied in detail because of occurrences of gold (Hubbard, 1975), and it is made up of two spatially, lithological and geochemically distinct groups of rocks, namely quartzite and granite-gneiss separated by the Ifewara fault.

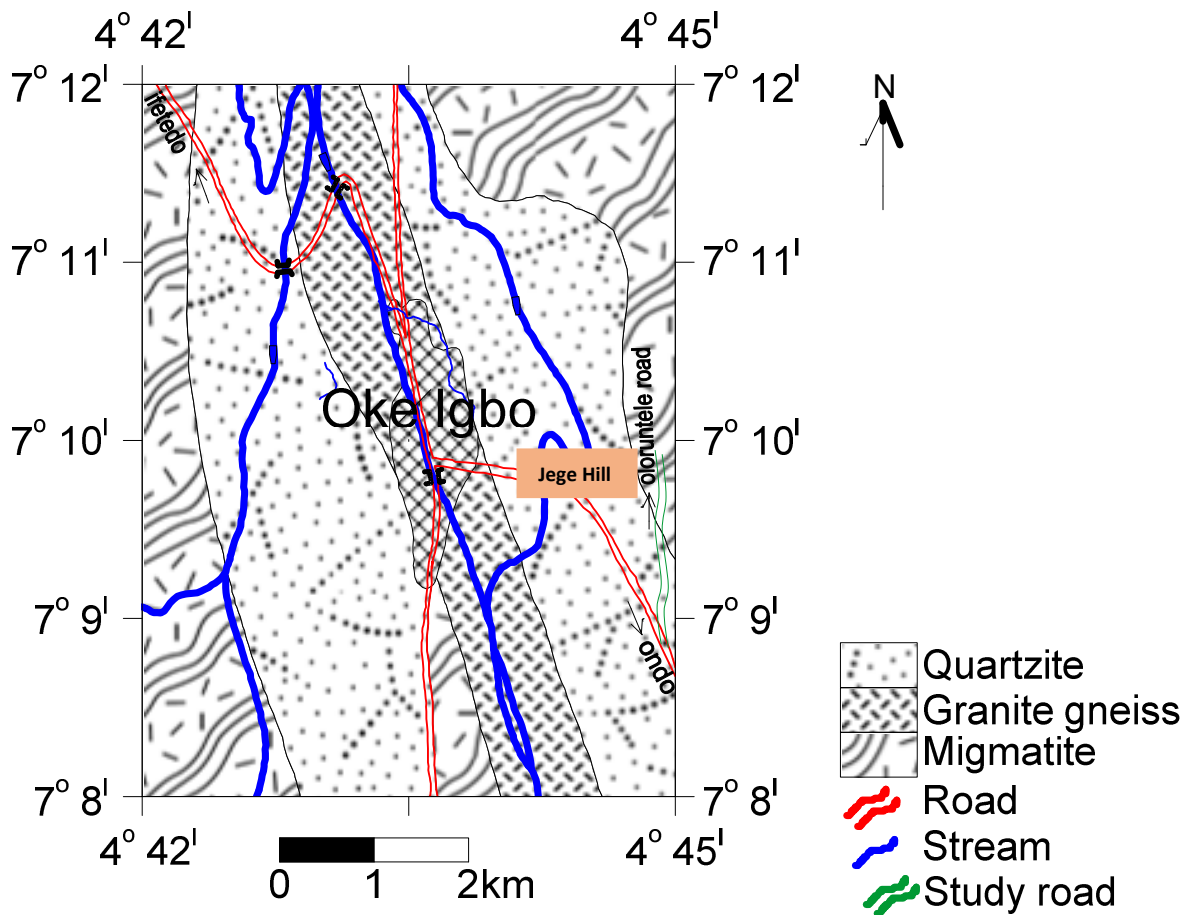


Figure 1: Geological Map of Oke Igbo, showing the Study Area Location (After Ikubuwaje, 2008)

The road investigated, exists within Oke-Igbo Local Government area of Ondo State in the Southwest of Nigeria and lies within longitudes of 693900 – 693700 E and latitudes 791900 – 791400 N. The study area lies entirely on the slopes of Jege hills that have witnessed major landslide in recent time (Akinlabi *et al.*, 2018). The elevation of the town varies between 700 m and 800 m above sea level (Figure 2). It lies within a broad valley, straddled on both sides by two rugged quartzite ridges with sharp, steep cliffs and precipitous slopes, while many isolated hills rise up to 1300 m above sea levels (Figure 3). Two rivers (Oni and Olori Rivers) drain the hilly landscape of the study area (Figure 4), while minor streams and streamlets, are enhanced by the steep slopes drain into these two rivers.

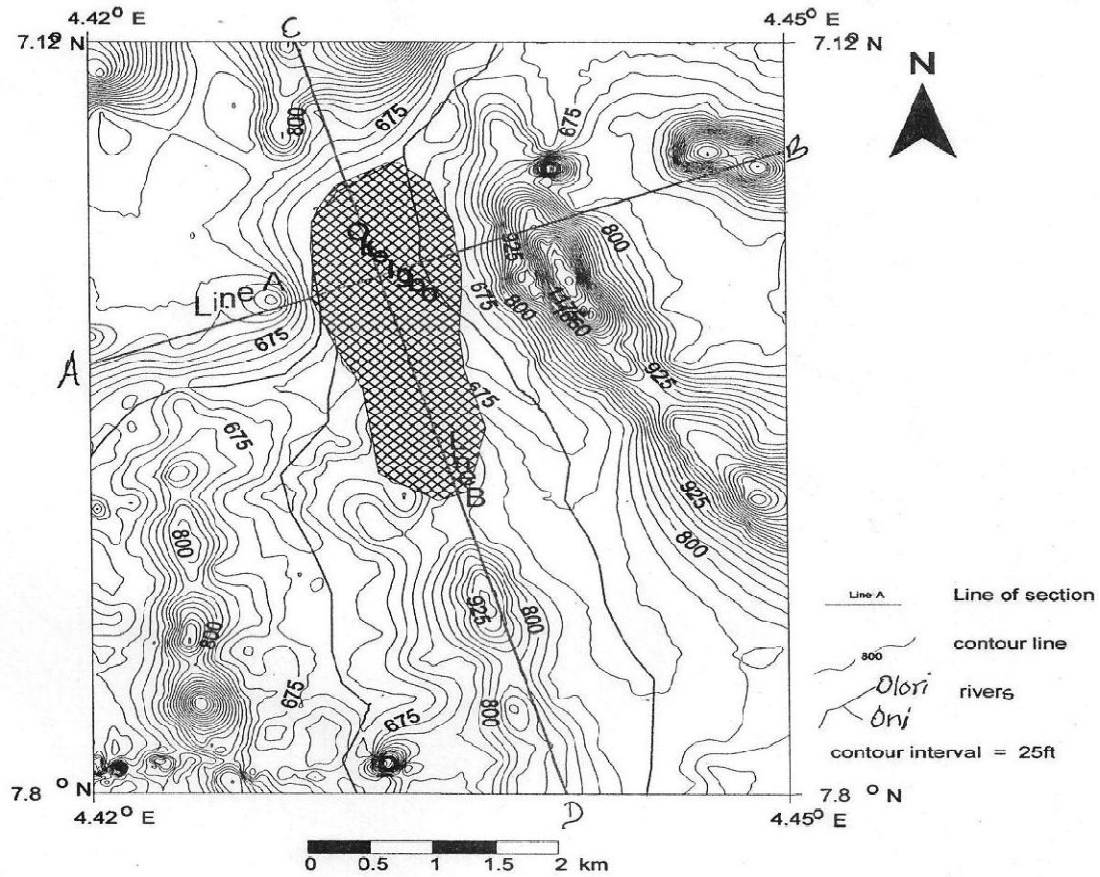


Figure 2: Topographic Map of Oke-Igbo (After Ikubuwajeet *et al.*, 2013)

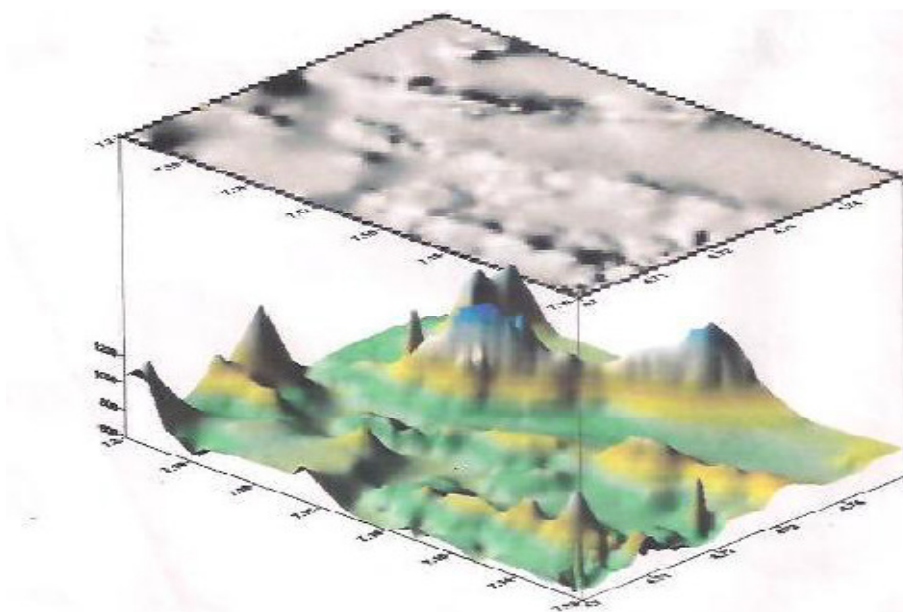


Figure 3: Geomorphology of Oke-Igbo (After Ikubuwajeet *et al.*, 2013).

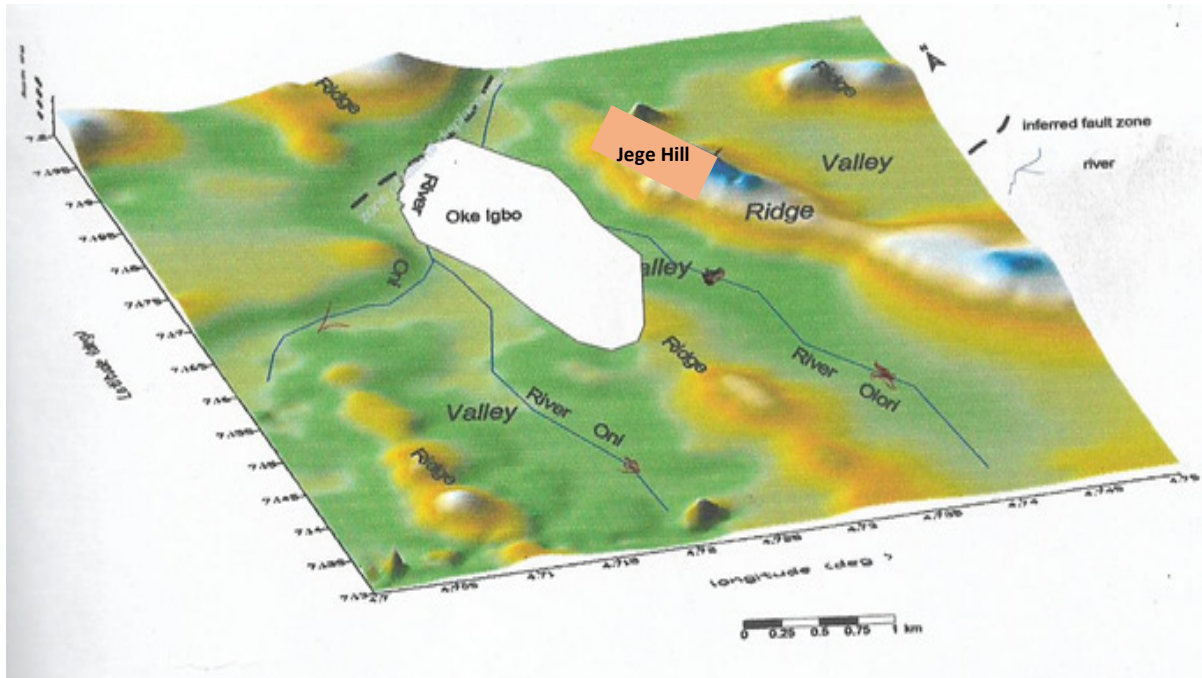


Figure 4: Drainage Map of Oke-Igbo (After Ikubuwaje, 2008)

The study area lies within the tropical rainforest zone of south-western Nigeria with abundance of rainfall in the wet season that span from April to October and becomes scanty or nil during the dry season (November to March). A single maximum rainfall distribution pattern is typical, however the rainfall variations during the wet season are sometimes with disparity due to the contributing effect of orographic rainfall. Vegetation is very thick in the rugged and inaccessible areas, where a delicate balance exists between vegetation, soil cover and land degradation, while within the town vegetation is very sparse.

The hydrological characteristics of the rocks around Oke-Igbo are influenced by the nature of the lithology whereby primary porosity and permeability are low in basement metamorphic regions with extensive faulting and fracturing that have made the quartzite in particular to become highly permeable. The rugged and undulating topography also favours directional flow of surface and groundwater. Clay, silt, sand and gravel constitute the main overburden, thus paving the way for groundwater migration and storage.

3.0 METHODOLOGY

3.1 Geophysical Surveys

The electrical resistivity method employed involved two field techniques, the vertical electrical sounding (VES) with the aids of Schlumberger array and combined horizontal profiling and vertical electrical sounding (2-D electrical imaging) using dipole-dipole configuration. Eight geophysical traverses were established across the studied road; each having a spread of 80 m across an unstable road segment of a length totalling 300 m (Figure 5).

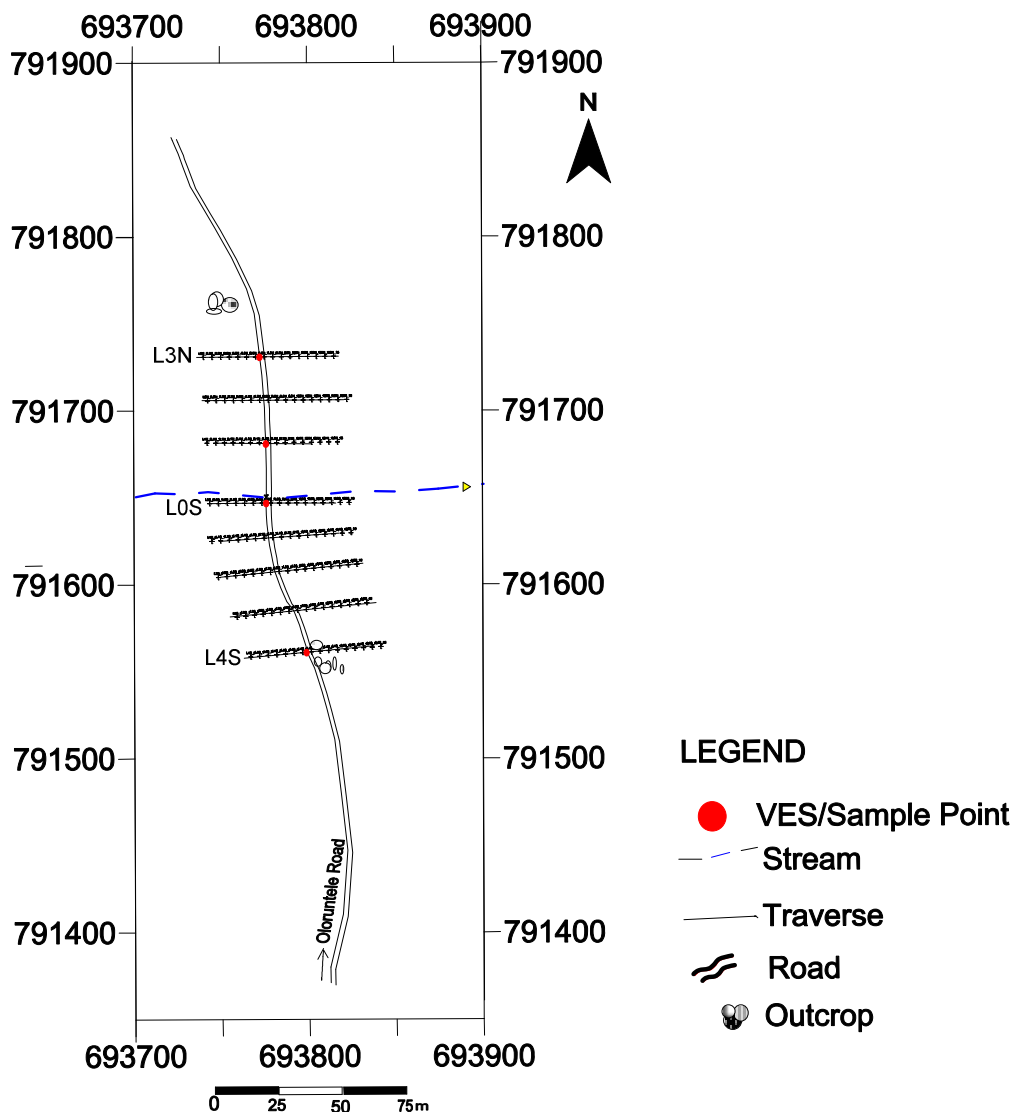


Figure 5: Field Data Acquisition Map of the Study Area

3.1.1 Combined Resistivity Profiling and Sounding (2D Electrical Imaging)

The combined resistivity profiling and sounding (CRPS) was conducted with the use of Schlumberger dipole-dipole electrode configuration across each traverse. The dipole-dipole array, first described by (Alpin, 1966) allows for the qualitative and quantitative characterisation of resistivity distribution within the subsurface in 2-dimensional sense. The inter electrode spacing of 5 m was adopted, while inter dipole expansion factor (n) was varied from 1 to 5 (Figure 6). The 2D inversion modelling of the dipole-dipole data was carried out using a software package known as DIPROTM. The 2D resistivity inversion can be carried out using the finite element method (FEM) or finite element difference (FED) mathematical inversion algorithm with smoothness constraint in alternative manner.

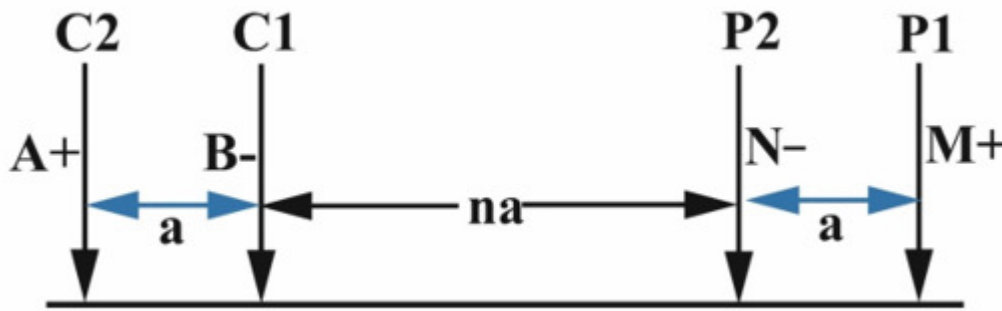


Figure 6: Schlumberger dipole-dipole Configuration

3.1.2 Vertical Electrical Sounding (VES)

The vertical electrical sounding (VES) that allows vertical expression of layer resistivity to be derived was adopted in order to characterise the vertical variation of the subsurface resistivity with depth at selected locations based on the results of the early CRPS conducted. In carrying out vertical electrical sounding, vertical variations in the ground apparent resistivity are measured with respect to a fixed centre of the array. Four (4) Vertical Electrical Sounding points were occupied across the study area using the Schlumberger array, while the current electrode spacing ($AB/2$) was varied from 1 to 100m. Sounding locations were at station 6, on Traverse L4s, L0S, L1N and L3N, which corresponds to 30 m distance on each traverse respectively specifically at the central positions of the road segment.

The apparent resistivity measurements at each station were plotted against electrode spacing on bi-logarithmic graph sheets. Partial curve matching was carried out for quantitative interpretation of the curves. The results of the partial curve matching (layer resistivities and thickness) were fed into the computer program, RESIST version 1.0 (Vander Velper, 1988) for the iterative forward modelling of the

VES data in order to improve the 1D inversion of the resistivity data. Geoelectric section along the road segment was then generated from the inverted 1D profiles from the VES results (layer resistivity and thickness values).

3.2 Geotechnical Investigation

Disturbed soil samples were collected at each of the VES locations at a depth not exceeding 1 m. The sample locations were at VES points located on Traverse L4S, L0S, L1N and L3N, which corresponded to 30 m distance respectively on each traverse. The soil samples were labelled **S1**, **S2**, **S3** and **S4** and the following laboratory tests were conducted on them.

3.2.1 Particle Size Distribution (PSD)

In order to classify a soil for engineering purposes, there is a need to have the knowledge of distribution of particles or grains' sizes in the soil mass. Sieve analysis was conducted in order to determine the grain size distribution of soils in the study area. It is a method of separating soil into fraction based on particle size. It is expressed quantitatively as the proportion by mass of various sizes of particles present in a soil. The results of the particle size analysis were used in soil classification. AASHTO Soil Classification System developed by the American Association of State Highway and Transportation Officials was used as a guide for the classification. Particle size distribution curves were also used in conjunction with graphically expressed particle-size limits to determine the suitability of the soils for road construction.

3.2.2 Liquid Limit Test

Liquid Limit Test was performed on the samples to determine the moisture content (LL) at which the sample would pass from a liquid state to a plastic state or the water content at which the soil starts to act as a liquid. The moisture content is an intrinsic property that can give information about the soil integrity or competency as foundation material.

3.2.3 Plastic Limit Test

The test was performed on the samples to determine the plasticity limit (PL) at which the sample would change from a plastic to a semisolid state. The moist soil is rolled into a thread of 3mm diameter and then the moisture content at which it crumbled obtained.

3.2.4 Plasticity Index (PI)

The plasticity index of the samples is the arithmetical difference between liquid limit and plastic limit value, it is the range of moisture content at which the soil is plastic. The index is used to predict or assess the expansivity of the soil. The lower the plasticity of a soil, the better is the engineering property of the soil. The PI was calculated using the formula;

$$PI = LL - PL \quad (1)$$

Where LL is liquid limit and PL is Plastic limit.

3.2.5 Shrinkage Limit Test

Mathematically linear shrinkage is calculated using the expression;

$$\text{Linear shrinkage (L.S)} = 1 - \frac{\text{Dry length}}{\text{Original length}} \times 100 \quad (2)$$

3.2.6 Hydraulic Conductivity Test (Falling Head Permeability Test)

In order to study the flow of water through the permeable soil samples and carry out stability analyses, the hydraulic conductivity of the soil samples (S1, S2, S3 and S4) was carried out to determine the coefficient of permeability of the samples. The falling head test was used, where water from a standpipe flows through the soil. The initial head difference h_1 at time $t = 0$ is recorded, and water is allowed to flow through the soil specimen such that the final head difference at time $t = t_2$ is h_2 .

The coefficient of permeability (K) is given by the expression:

$$k = 2.303 \frac{aL}{A \Delta t} \text{Log}_{10} \frac{h_1}{h_2} \quad (3)$$

3.2.7 Compaction Test (Standard Proctor)

Compaction test was carried out on the soil samples (S1, S2, S3 and S4) to evaluate the compaction characteristics and variation of dry density with moisture content. The main objective is to determine the optimum moisture content (OMC) and maximum dry density (MDD) of the samples for a specified compaction effort by the standard proctor compaction method. The Standard Proctor Compaction was carried out in accordance with BS 1377: Part 4 (1990): 3.3. Soils were compacted in three layers using a 2.5kg rammer and 25 blows with a 3000cm³ mould. The moisture content and dry density acquired were used to produce the compaction curve from which MDD and OMC are obtained.

4.0 DISCUSSION OF RESULTS

4.1 Geophysical Investigation

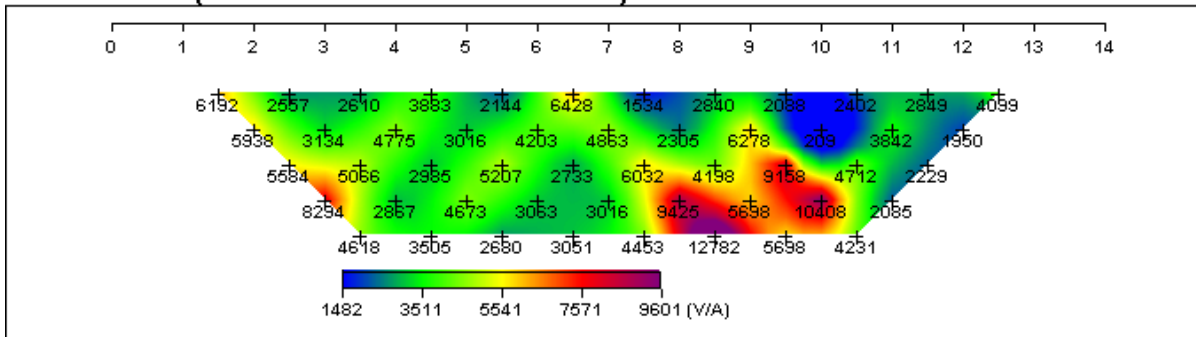
4.1.1 Resistivity Imaging

Results obtained from the resistivity imaging conducted along the various traverses are displayed as colour images of resistivity distribution within the subsurface that allows for structural evaluation of the subsurface from the sections generated. The resistivity sections indicated the pseudo section of the raw data, the pseudo section of the theoretical data that revealed the precision and accuracy of data acquired in representing the ideal resistivity distribution along the traverse and the inverted resistivity section; 2D resistivity structure that give the effective resistivity distribution of the near surface geology along the traverse.

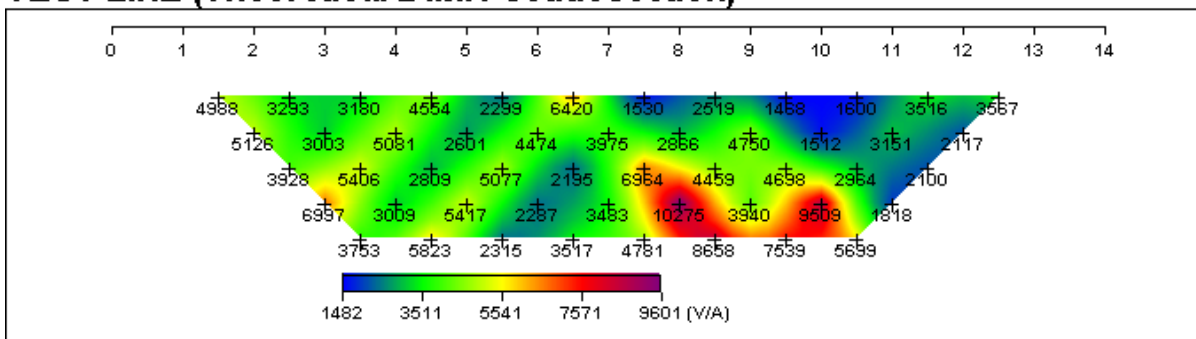
Figure 7 shows the 2D resistivity structure from the inverted CRPS data along traverse L3N. An outcrop of schistose quartzite is located north of the traverse with an offset of about 2 m, having low weathering impact. The thinness of the topsoil and relatively high layer resistivity suggests that the area is competent in general, but deeply eroded causing development of gully erosion at the road sides. The resistivity structure shows an expression of suspended bedrock to the east of the traverse and easterly dipping surface characterized by low resistivity that is diagnostic of lateritic materials found within the farmland in the study area. The topsoil varies in thickness ranging from about 2 – 5 m and development of eroding surface might result in weakening and reduction in the competency of the subsurface material in the area.

In Figure 8, the dipole-dipole raw data and theoretical data pseudo sections along with the generated 2D resistivity structure for the CRPS data collected along the traverse L2N are displayed. This traverse is characterised by similar topographic appearance similar to the L1N section, with thin topsoil underlying a highly weathered zone. A suspected fracture zone characterised by decreasing low resistivity values with depth at a distance between 35 m and 40 m was identified as weak zone along the traverse. This might be a major source of concern during the road construction. Along the fault zone and the undulation of the indurated quartzite bodies, there is possibility of silica leaching off the schistose quartzite ridge along the fractures and joint systems in the study area. The topography difference between the centre point along the road segment and ground level across the traverse line is between 0 m and 5 m, though the section of the road segment is relatively flat.

TEST LINE (Field Data Pseudosection)



TEST LINE (Theoretical Data Pseudosection)



TEST LINE (2-D Resistivity Structure)

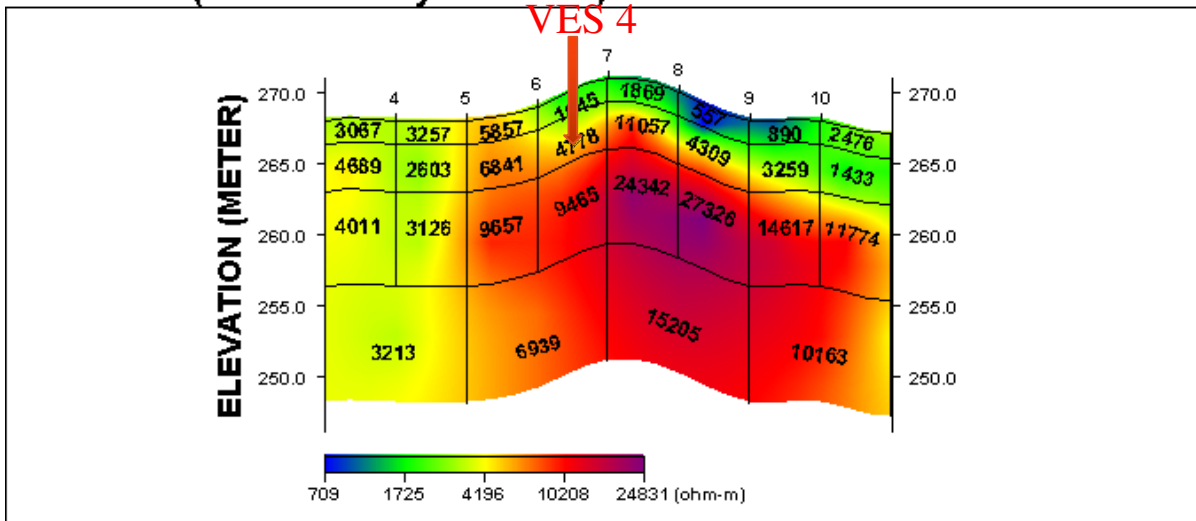
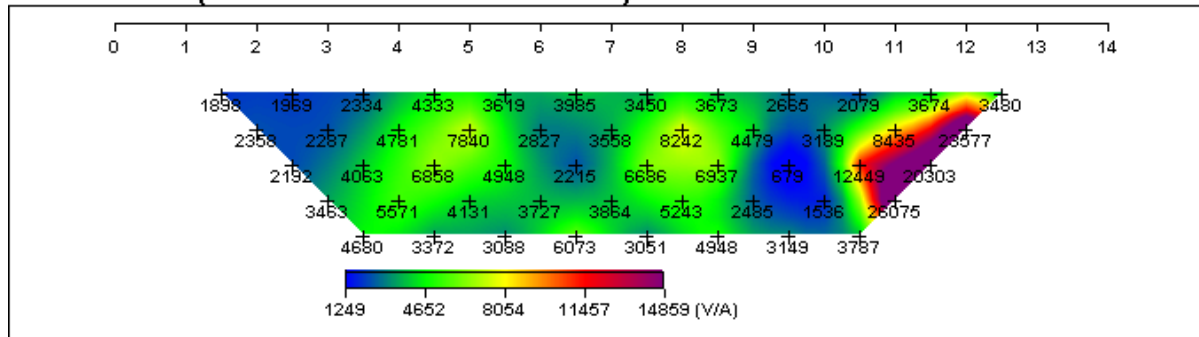
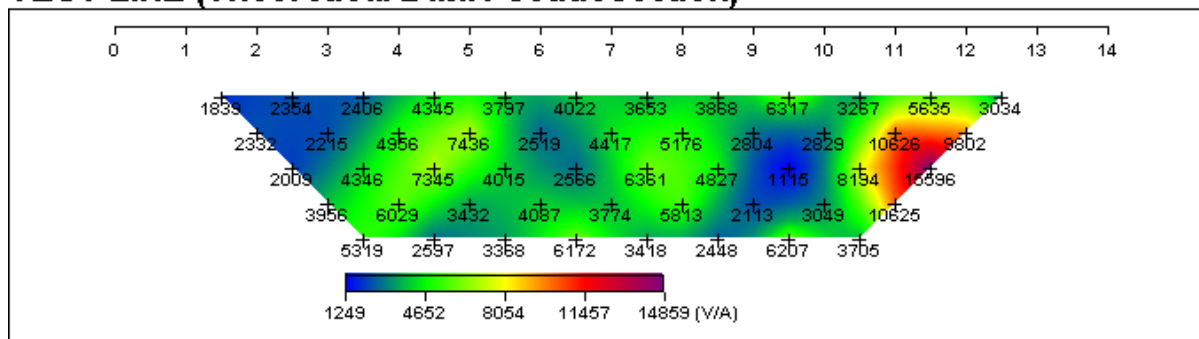


Figure 7: CRPSData Inversion showing the Dipole-dipole (2D) Resistivity Structure along Traverse L3N (W-E).

TEST LINE (Field Data Pseudosection)



TEST LINE (Theoretical Data Pseudosection)



TEST LINE (2-D Resistivity Structure)

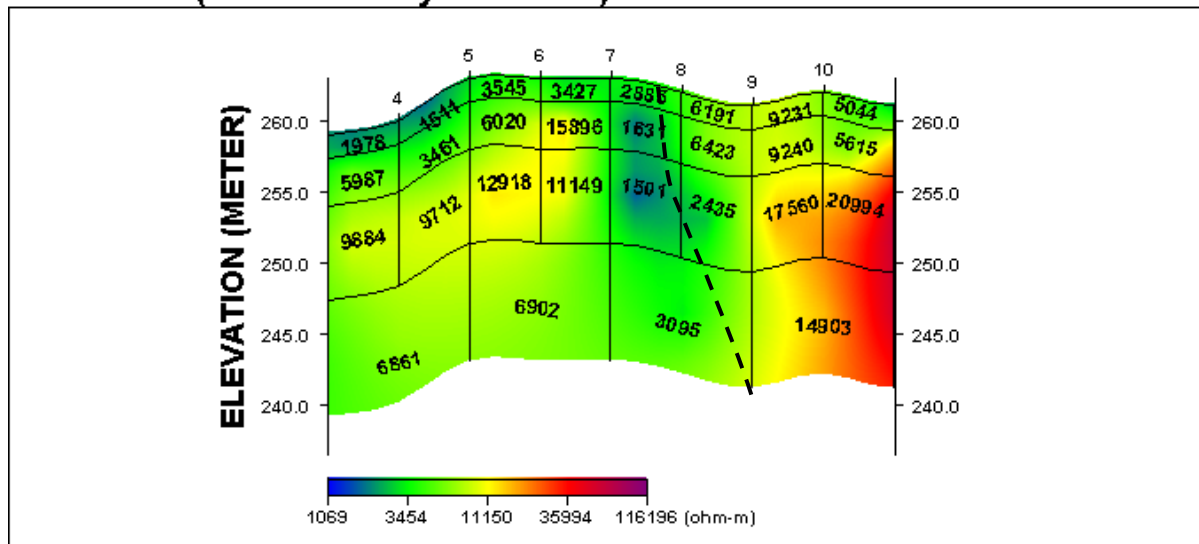


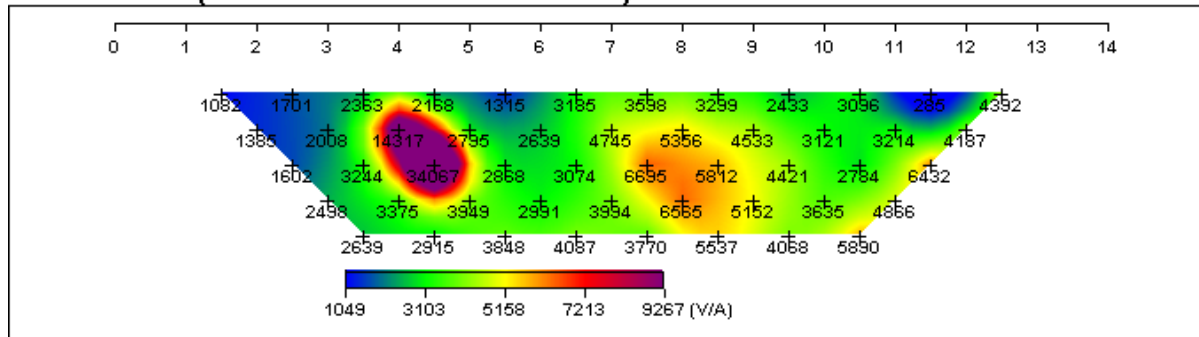
Figure 8: CRPSData Inversion showing the Dipole-dipole (2D) Resistivity Structure along Traverse L2N (W-E).

Figure 9 shows the results obtained from the inversion of the CRPS data acquired along the Base Line traverse labelled L1N that is made across the road segment a distance of 30 m north of the bridge over the river channel along the investigated road segment in the study area. From the 2D resistivity structure, the topography along the section generally undulating with respective elevation difference of the ground level across the traverse and centre point of the road ranging from 0 to 6 m. Although, the topography appears to be relatively flat close to the road segment, there will be a need for proper water channelling at the sides of the road for proper draining of the area.

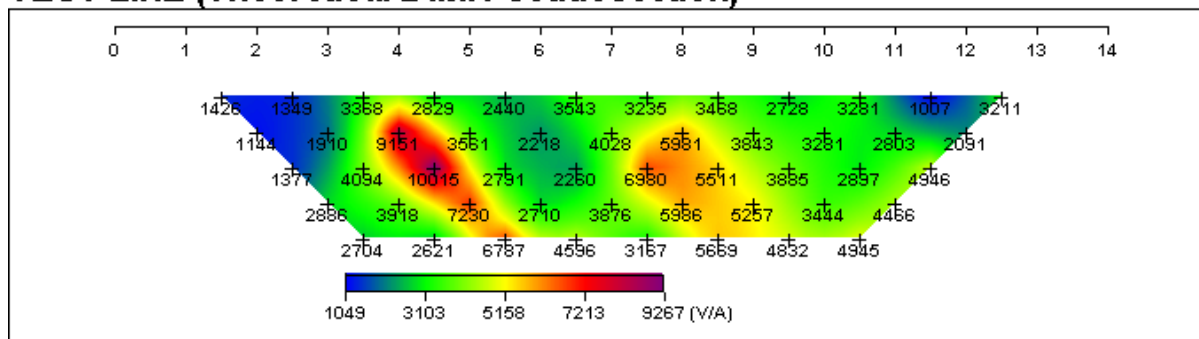
The results obtained from the inversion of the CRPS data acquired along the Base Line traverse labelled LOS that is situated a distance of about 5 m south of a bridge over a major river channel along the investigated road segment in the study area are shown in Figure 10.

The 2D resistivity structure depicts three geologic layers as reflected in the colour tones, which include topsoil (bluish colour), weathered layer (greenish to yellowish colour) and the fresh basement (reddish to magenta colour). The topsoil thickness varies from 0 to 2 m with the resistivity varying between 930 Ohm-m and 2,266 Ohm-m characteristic of resistive materials, which is suspected to be an indurated quartzite material from the field observation of the outcropped ridges in the area. The second layer is the presumed weathered layer with resistivity varying between 1,837 Ohm-m and 9,625 Ohm-m, having thickness ranging from 5 to 7.5 m. The second layer appears to outcrop at distance of about 20 – 27 m westward and 44 – 80 m eastward of the traverse. The underlying layer which is considered as fractured bedrock (basement rock) has resistivity values that vary from 5,324 to 13,865 Ohm-m. The depression observed to the western section is identified as the expression of faulting in the NW-SE direction that cut across the road segment. The surface topography is generally undulating, with topography difference between the maximum and lowest points along traverse and ground level at the centre of the road segment running south to north lying between 0 m and 2 m along the traverse. The implication of this is that for the road to be stabilised, there should be cutting and in-filling with competent materials at the section of the road in the W-E direction and across the entire unstable segment. Geologically, the topsoil and weathered materials appear to be relatively stable owing to the high resistivity value. It can therefore be concluded that the subsoil on which traverse LOS is founded is generally competent.

TEST LINE (Field Data Pseudosection)



TEST LINE (Theoretical Data Pseudosection)



TEST LINE (2-D Resistivity Structure)

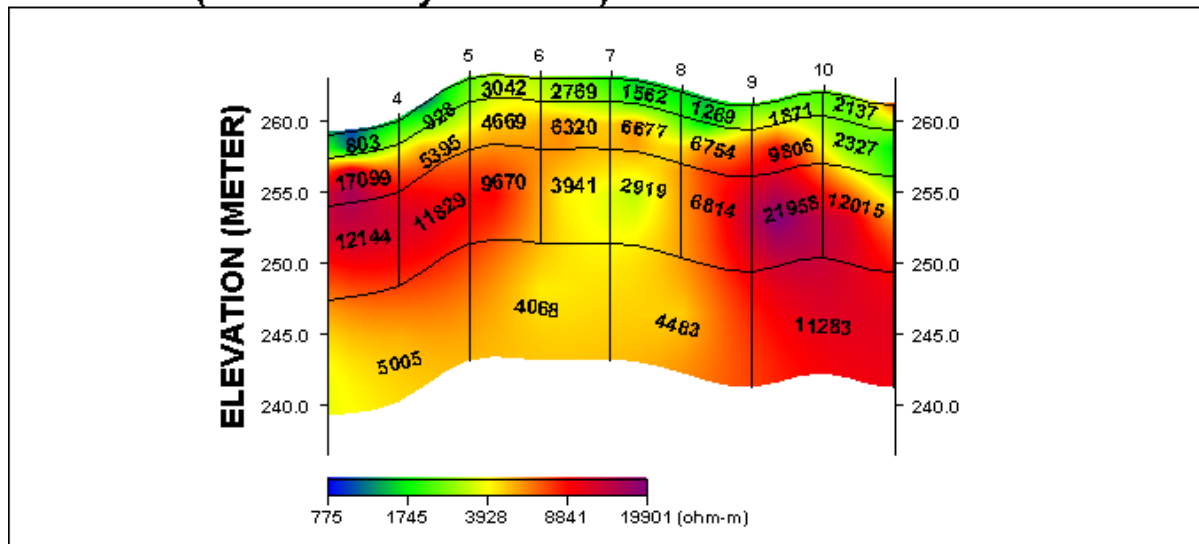
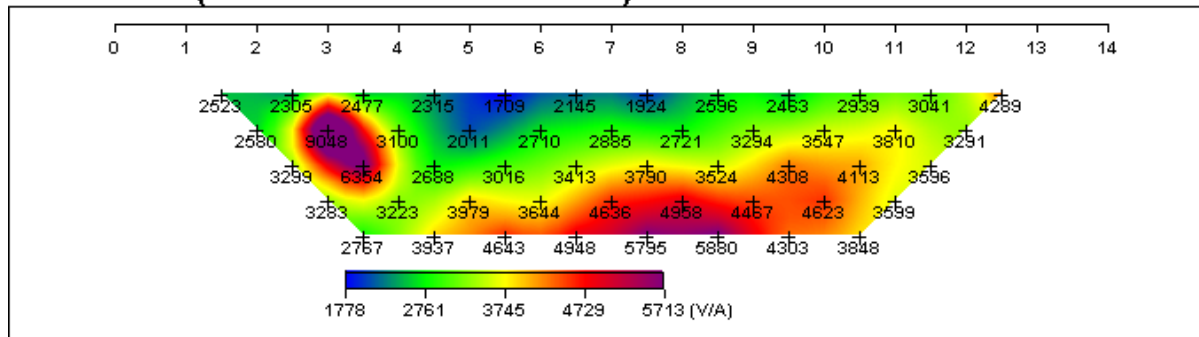
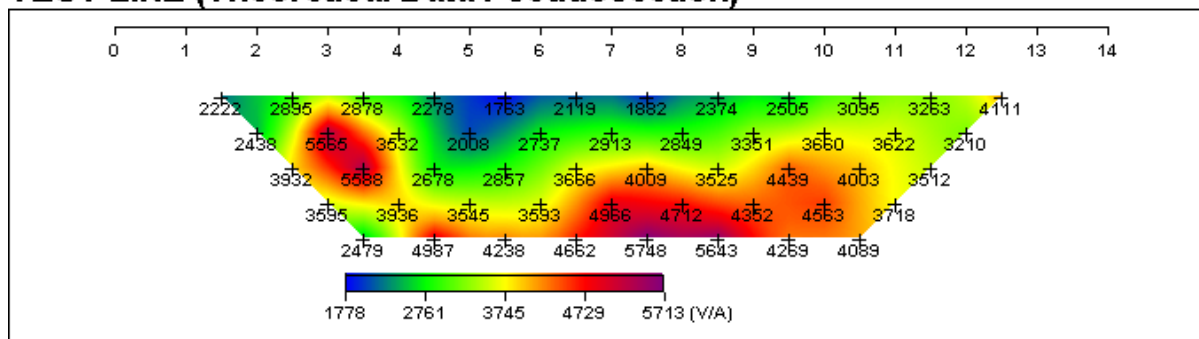


Figure 9: CRPSData Inversion showing the Dipole-dipole (2D) Resistivity Structure along Traverse L1N (W-E)

TEST LINE (Field Data Pseudosection)



TEST LINE (Theoretical Data Pseudosection)



TEST LINE (2-D Resistivity Structure)

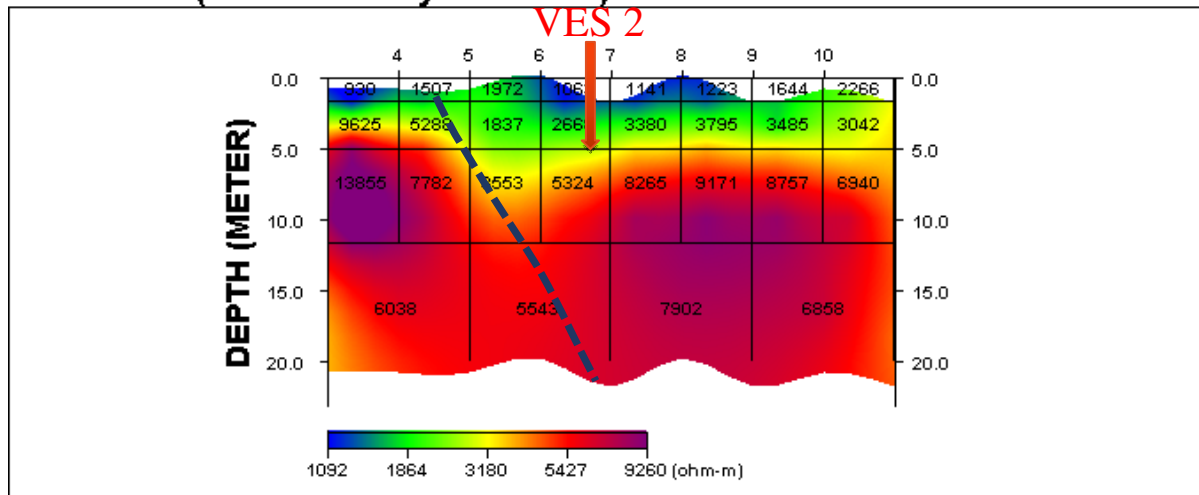


Figure 10: CRPSData Inversion showing the Dipole-dipole (2D) Resistivity Structure along Traverse LOS (W-E)

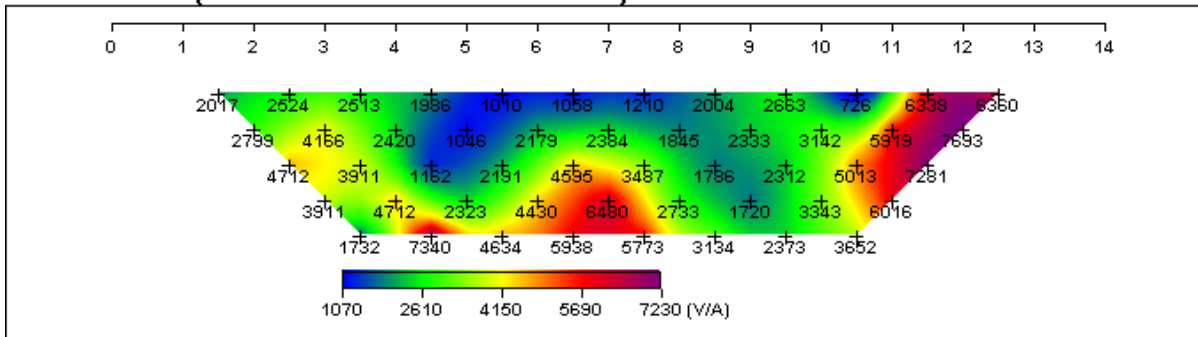
Reduction in resistivity values with depth observed in the 2D resistivity section, suggest that the uplift of the bedrock along the traverse has resulted in the infiltration of the underlying indurated quartzitic rock by surface runoff through joints and fissures.

The weathered layer is fairly thin across the traverse with most of the topsoil eroded. Geologically, this section is presumed to be fairly competent, but overtime due to degradation the possibility of the section becoming weaker is much higher if the road segment is not properly drained.

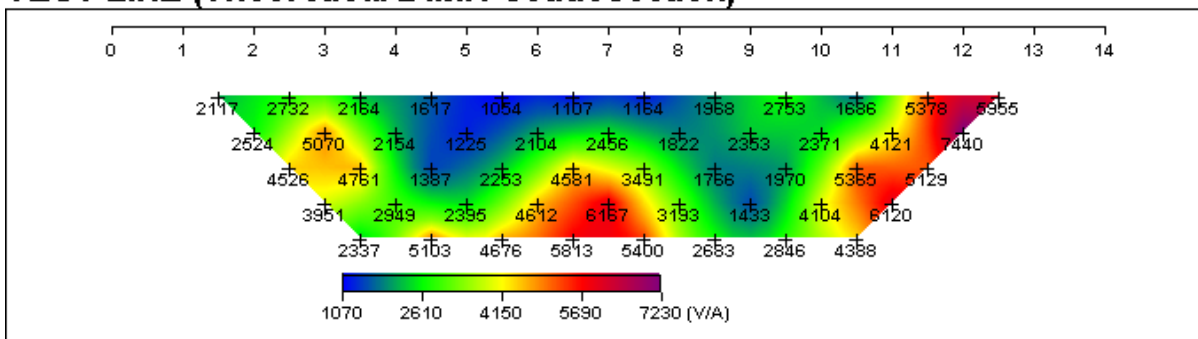
Figure 11 shows the results obtained from the inversion of the CRPS data acquired along traverse L1S. The characteristic lithological sequence includes very thin topsoil (indicated by bluish to greenish colour tone), weathered layer (greenish/yellow colour tone) and the fresh bedrock (reddish to magenta colour tone). The topsoil thickness varies from 0 to 2 m with the resistivity ranging from 376 to 5467 Ohm-m, characteristic of resistive weathered quartzite material. Beneath the topsoil is a thin weathered layer with resistivity between 1079 Ohm-m and 5454 Ohm-m, while the underlying layer is considered as fresh bedrock characterized by high resistivity (3,683 – 19,628 Ohm-m). The topography difference between the point on the centre of the road and ground level along the traverse is between 0 and 5 m. However, the section of the road along the traverse appears to be relatively flat and the topsoil made of loose sand.

Figure 12 shows the inversion results of the CRPS data acquired along traverse L2S with the 2D resistivity structure revealing three geologic layers, which include resistive topsoil (greenish colour tone), weathered layer (yellowish colour tone) and fresh bedrock (reddish/purple colour tone). The topsoil is thin and less than 3 m thick with high layer resistivity (1,246 – 4,142 Ohm-m). The weathered layer is characterized by resistivity value ranging from 1,220 – 4,906 Ohm-m, with a suspected low resistive (338 Ohm-m) indicative of cavity, likely to be infilled with sandy materials at distance from 30 to 35 m. The cavity could probably be associated to shallow groundwater channel.

TEST LINE (Field Data Pseudosection)



TEST LINE (Theoretical Data Pseudosection)



TEST LINE (2-D Resistivity Structure)

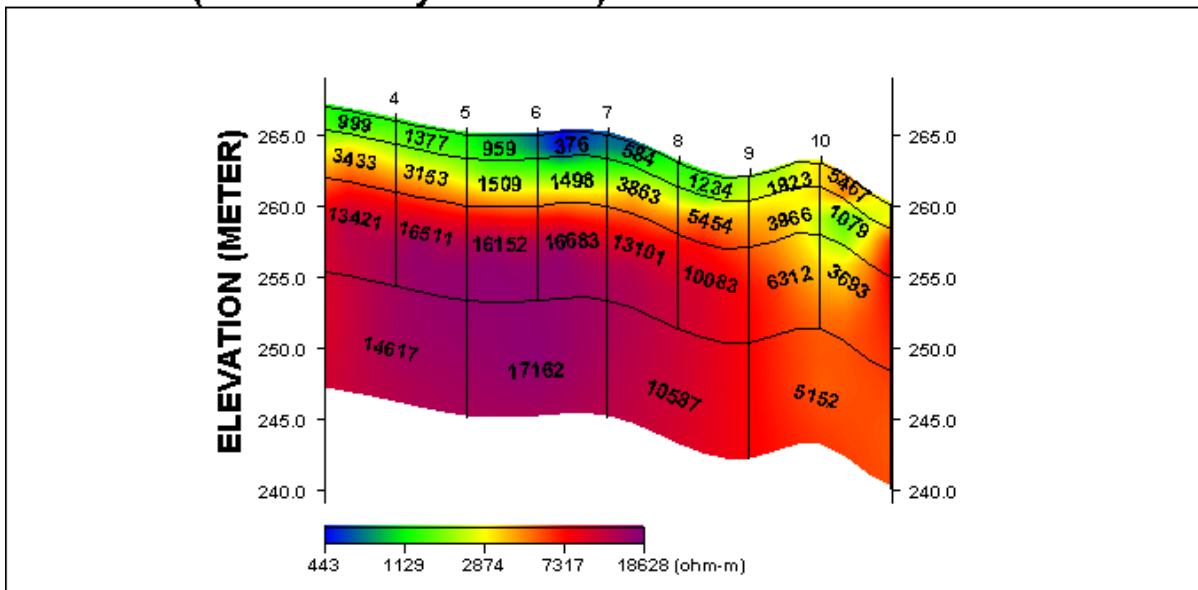
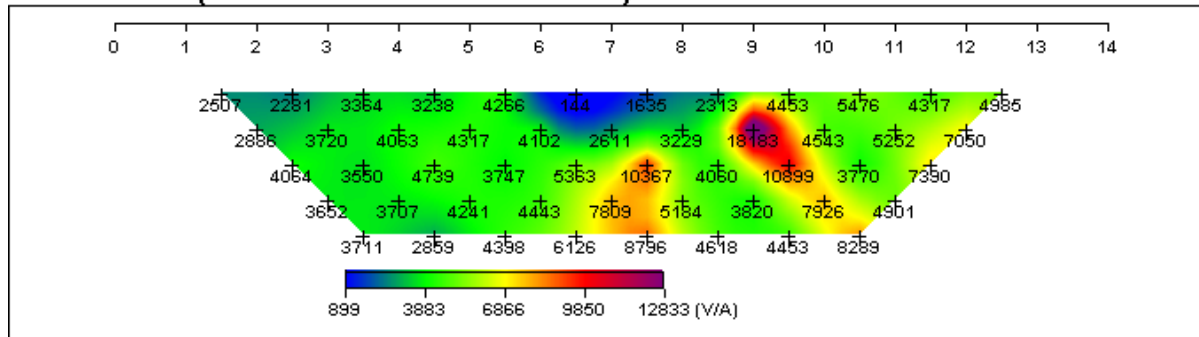
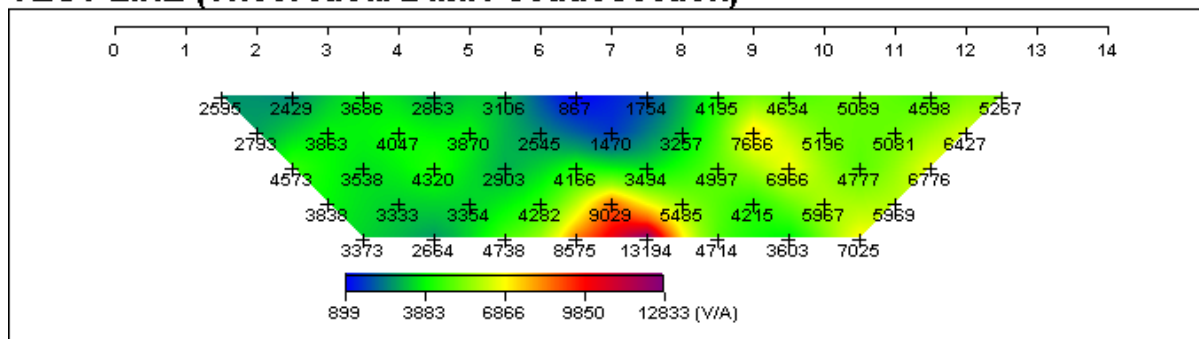


Figure 11: CRPSData Inversion showing the Dipole-dipole (2D) Resistivity Structure along Traverse L1S (W-E)

TEST LINE (Field Data Pseudosection)



TEST LINE (Theoretical Data Pseudosection)



TEST LINE (2-D Resistivity Structure)

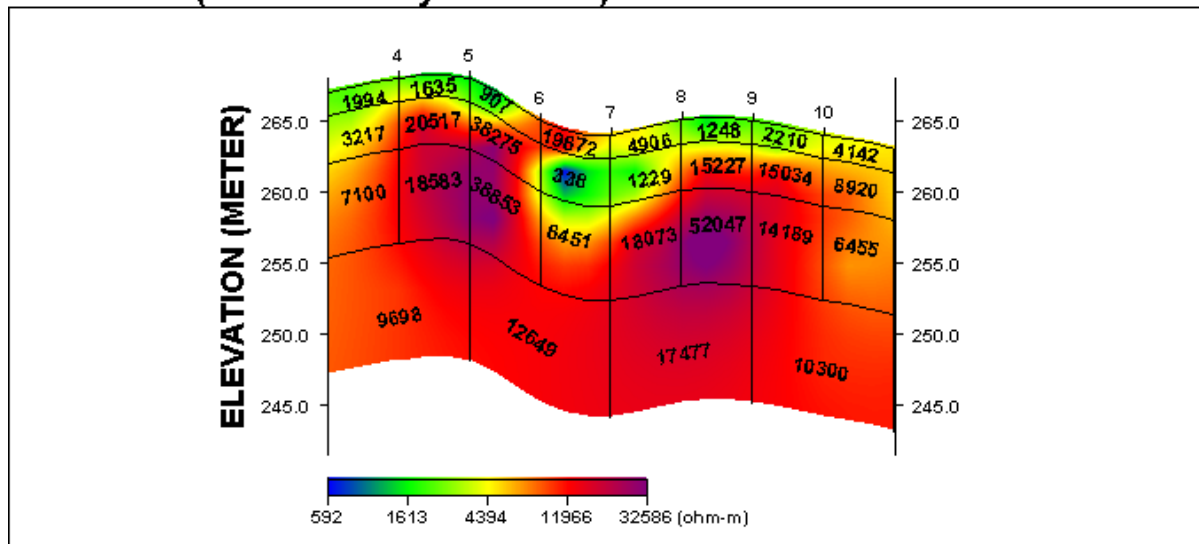


Figure 12: CRPSData Inversion showing the Dipole-dipole (2D) Resistivity Structure along Traverse L2S (W-E)

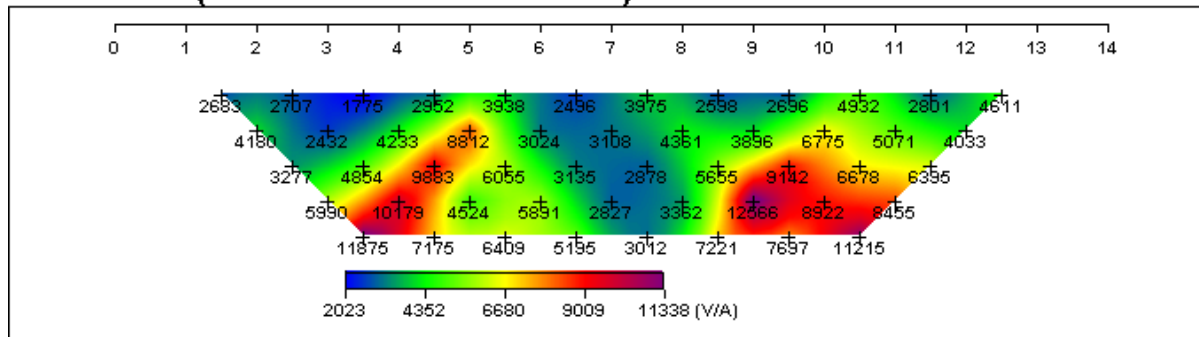
Due to the undulating topography of the profile, there will be a need for soil stabilisation and infilling at distance of 25 to 55 m in order to improve the sub-grade materials at this location.

In Figure 13, the 2D resistivity structure along traverse L3S shows a subsurface sequence with a topsoil having a thickness of about 2 m with high resistivity and a uniformly thin weathered layer (less than 1 m thick) characterized by resistivity ranging from 1,185 – 5,504 Ohm-m (bluish/greenish colour) and resistive bedrock with resistivity varying from 9,915 – 32,586 Ohm-m (reddish to magenta colour tone). Around the central part at distance of 20 to 25 m along the section, the impact of erosion from the surface run-off is presumed to have resulted in the depression observed, characteristic of low resistive material suggesting increase in water content of the weathered bedrock. The depression is observed to be an extension of the near surface cavity observed on traverse L2S, 30 m northward.

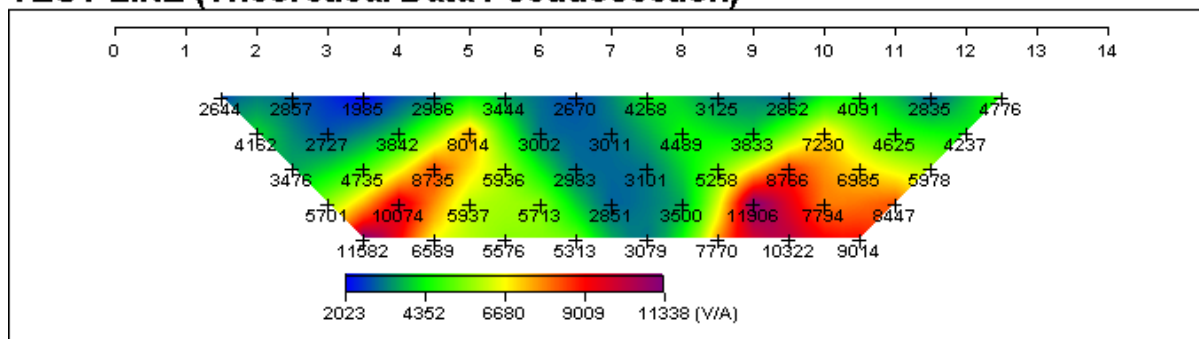
In Figure 14, the inversion results of the CRPS data acquired along traverse L4S shows the 2D resistivity structure with fairly undulating surface, characterized by 3-layer lithologic framework. The topsoil is generally resistive with resistivity value ranging from 1940 – 2726 Ohm-m and thickness less than 1 m. The weathered layer is also thin along the section with thickness of about 0.2 – 1 m.

The resistivity of the second layer ranges from 3,996 – 8,003 Ohm-m, while the bedrock is highly resistive with resistivity values in the range of 5,071 – 2,1012 Ohm-m, this traverse that is presumed to be more stable due to the generally high resistivity of the section. However, a localized low resistivity linear feature at 30 m (close to station 6) away from the west end is suggested to be vertically fractured quartzite extending to the surface with characteristic resistivity from 2,670 – 5,513 Ohm-m. Generally, from the 2D resistivity structure, it shows that along this section, the subsurface is competent and can serve as a good subgrade.

TEST LINE (Field Data Pseudosection)



TEST LINE (Theoretical Data Pseudosection)



TEST LINE (2-D Resistivity Structure)

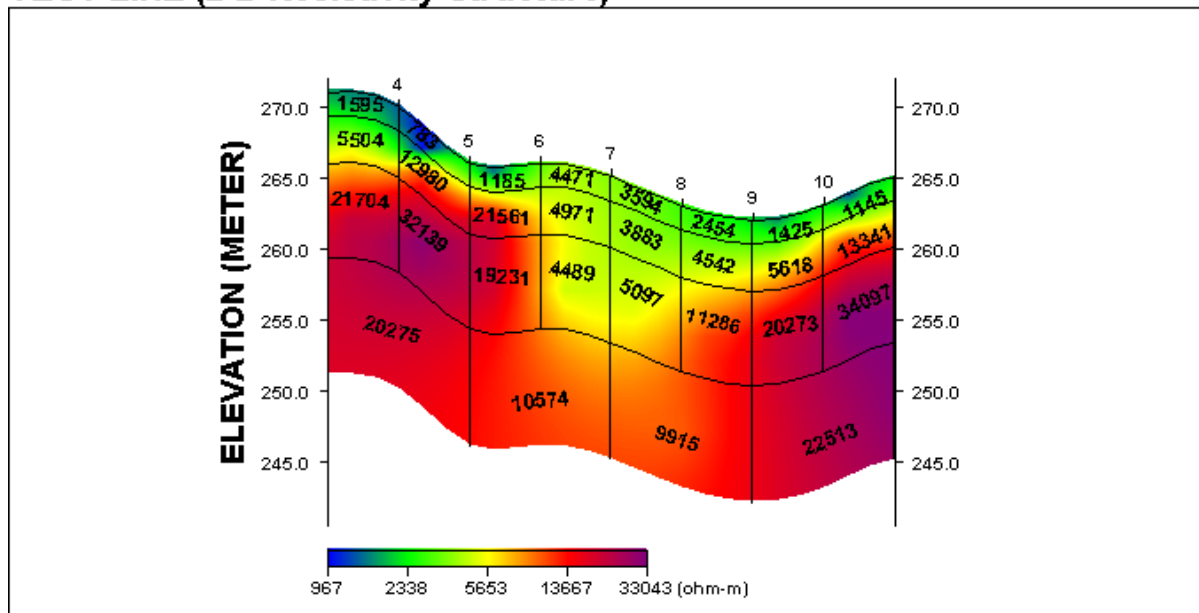
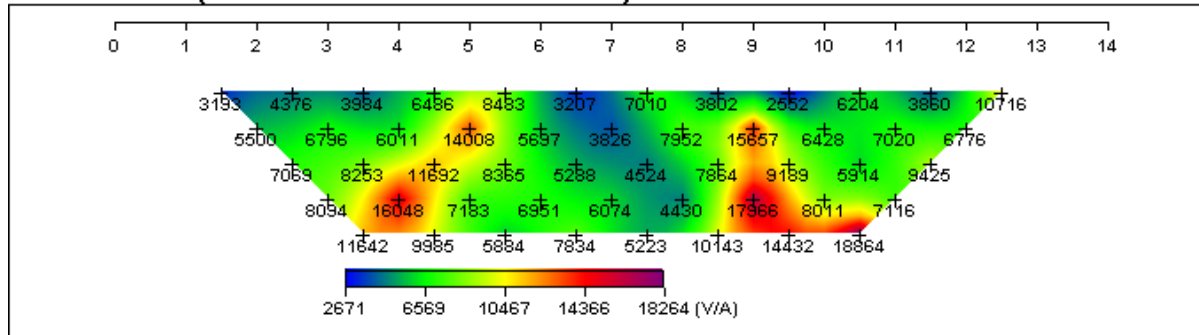
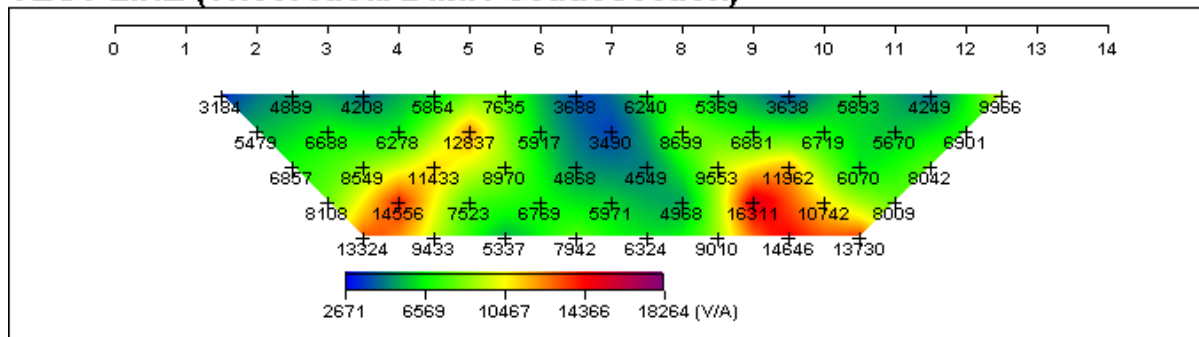


Figure 13: CRPSData Inversion showing the Dipole-dipole (2D) Resistivity Structure along Traverse L3S (W-E)

TEST LINE (Field Data Pseudosection)



TEST LINE (Theoretical Data Pseudosection)



TEST LINE (2-D Resistivity Structure)

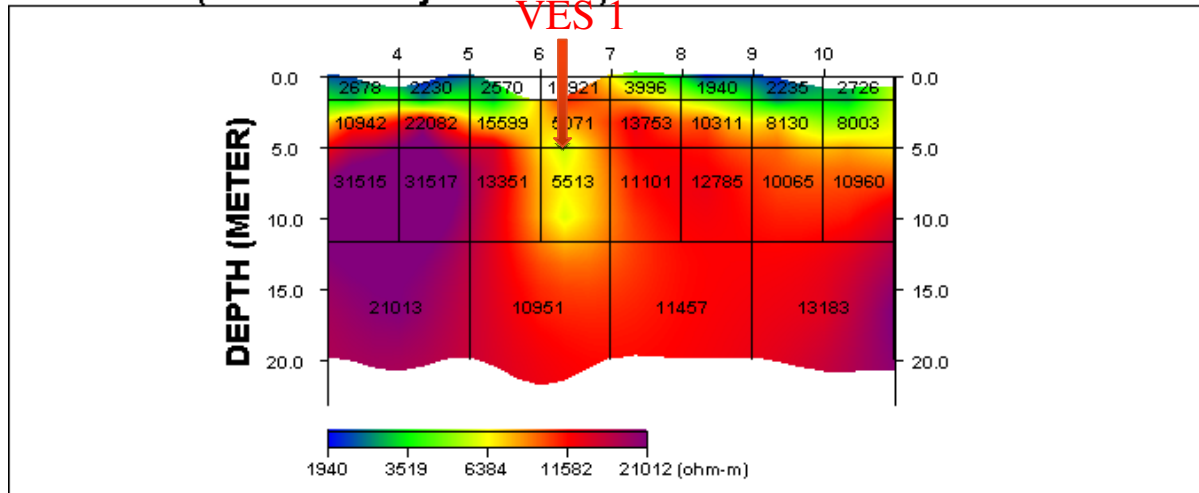


Figure 14: CRPSData Inversion showing the Dipole-dipole (2D) Resistivity Structure along Traverse L4S (W-E)

4.1.2 Vertical Electrical Sounding

Table 1 shows the summary of the results of the vertical electrical soundings obtained from the 1D inversion of the field data at the four sounding locations, all producing a type-KH curve characterized by four lithologic units. The interpreted VES curves are presented in Figures 15 - 18. The curve type represents a subsurface condition in which there is an increase in resistivity from topsoil to the weathered layer and a decrease in resistivity from the weathered layer to the fractured layer where it increases to the fresh bedrock. The curve type is typical of a succession of relatively high resistivity weathered layer disrupted by a relatively low resistivity layer (Fractured bedrock). The trend observed suggests increase in compaction of the subsoil from the topsoil down to the bedrock, despite the increase in water content of the weathered layer due to groundwater recharge in the area.

In order to evolve a subsurface geological model at the investigated location, the results of the VES interpretation results were used to prepare a 2D geoelectric section (Figure 19). The geoelectric sequence obtained gives respective layer resistivity values and thickness, where the section revealed four geoelectric/geologic subsurface layers comprising the topsoil, weathered layer, fractured bedrock and fresh bedrock. The topsoil varies in composition from leached sand to clayey sand or laterite with resistivity varying from 325 to 1883 Ohm-m, while its thickness varies between 0.8 m and 1.6 m.

Table 1: Summary of the VES Interpretation Results

VES Number	Curve Type	Number of Layers	Resistivity Value (Ωm)	Thickness (m)	Lithological Characteristics
1	KH	4	1542.8	0.8	Topsoil
			3661.4	17.4	Weathered layer
			1627.5	5.5	Fractured Bedrock
			6447.3		Fresh Bedrock
2	KH	4	325.3	1.1	Topsoil
			11306.4	9.6	Weathered
			3722.5	10.9	Fractured Bedrock
3	KH	4	7723.2		Fresh Bedrock
			1574.9	1.6	Topsoil
			7965.1	9.3	Weathered
4	KH	4	2444.8	14.7	Fractured Bedrock
			10989.3		Fresh Bedrock
			1882.8	1.6	Topsoil
4	KH	4	4446.4	8.7	Weathered
			2092.9	12.9	Fractured Bedrock
			7515.1		Fresh Bedrock

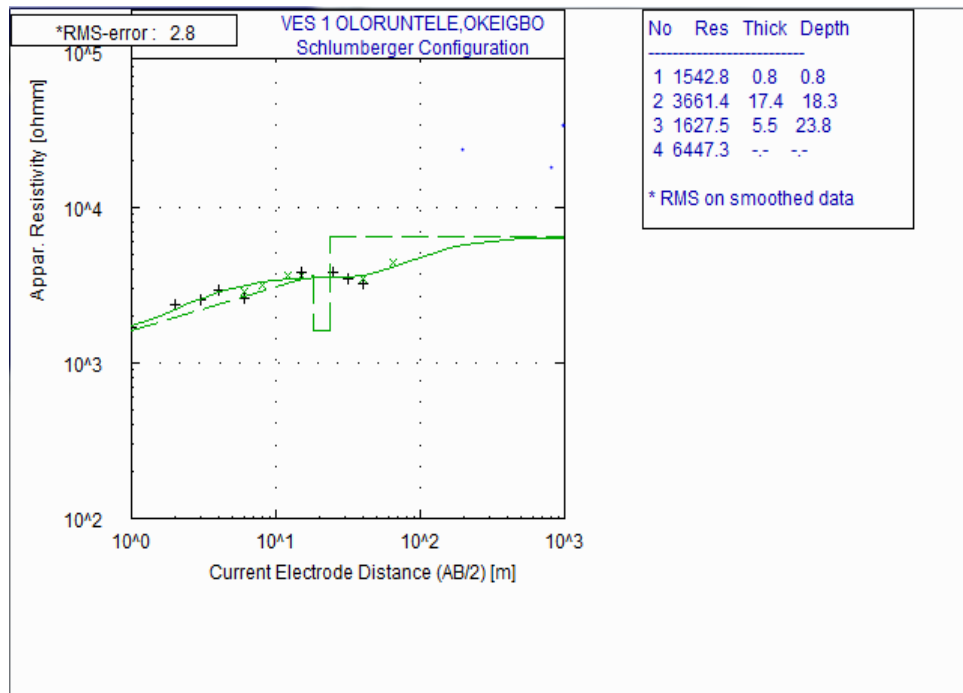


Figure 15: Curve Type Obtained at VES 1 along the Study Road

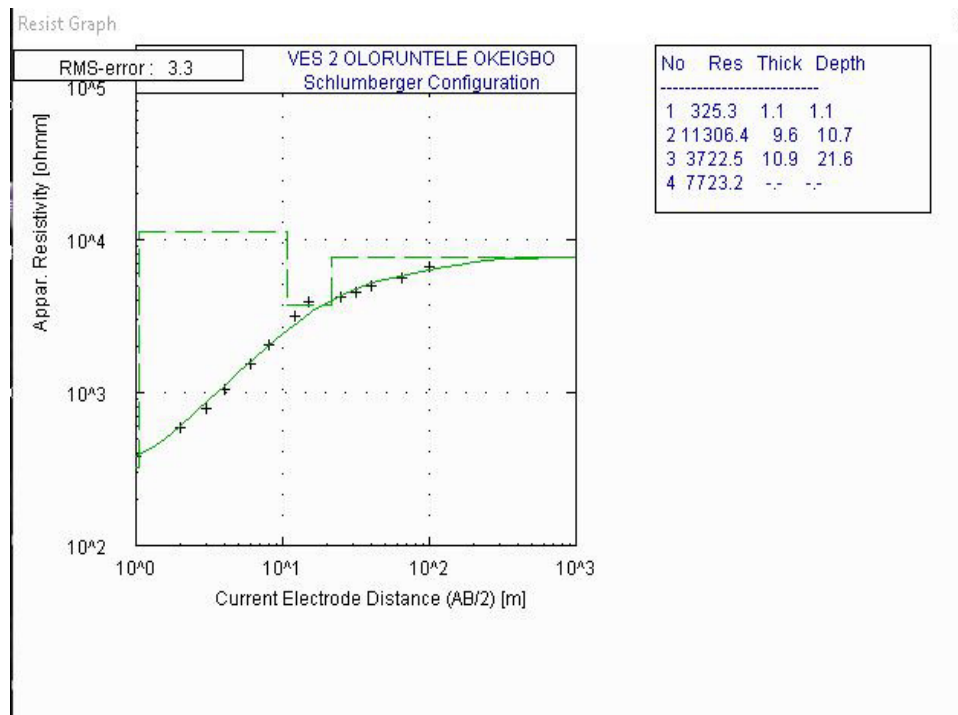


Figure 16: Curve Type Obtained at VES 2 along the Study Road

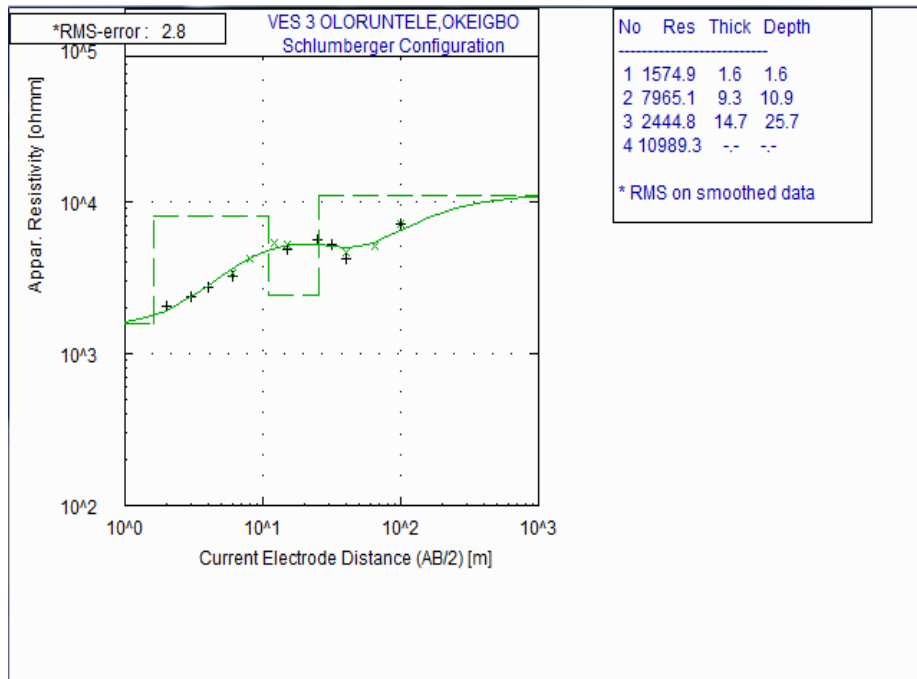


Figure 17: Curve Type Obtained at VES 3 along the Study Road

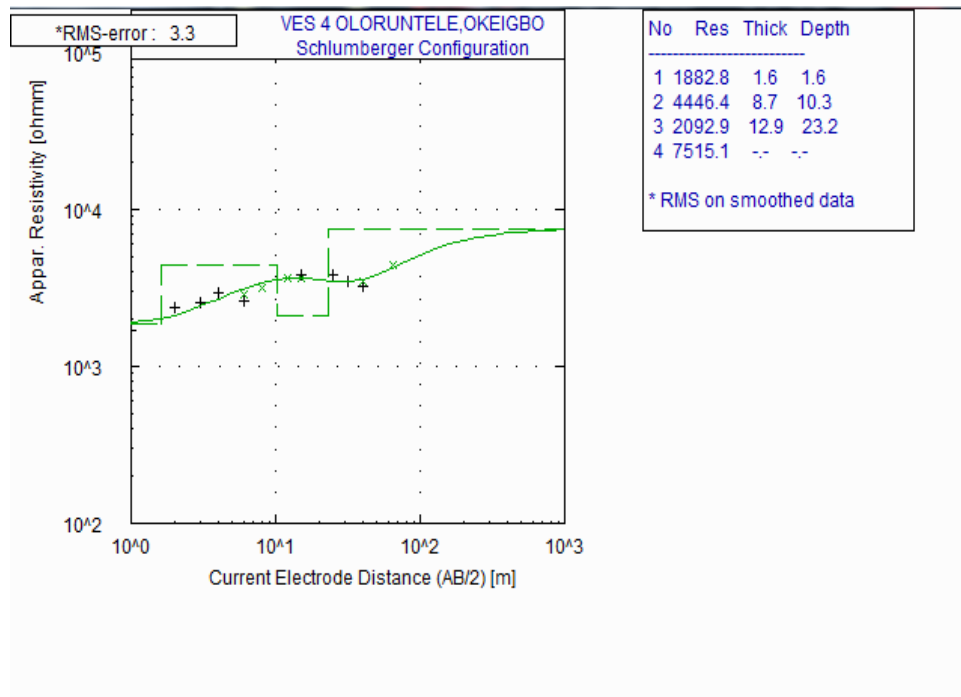


Figure 18: Curve Type Obtained at VES 4 along the Study Road.

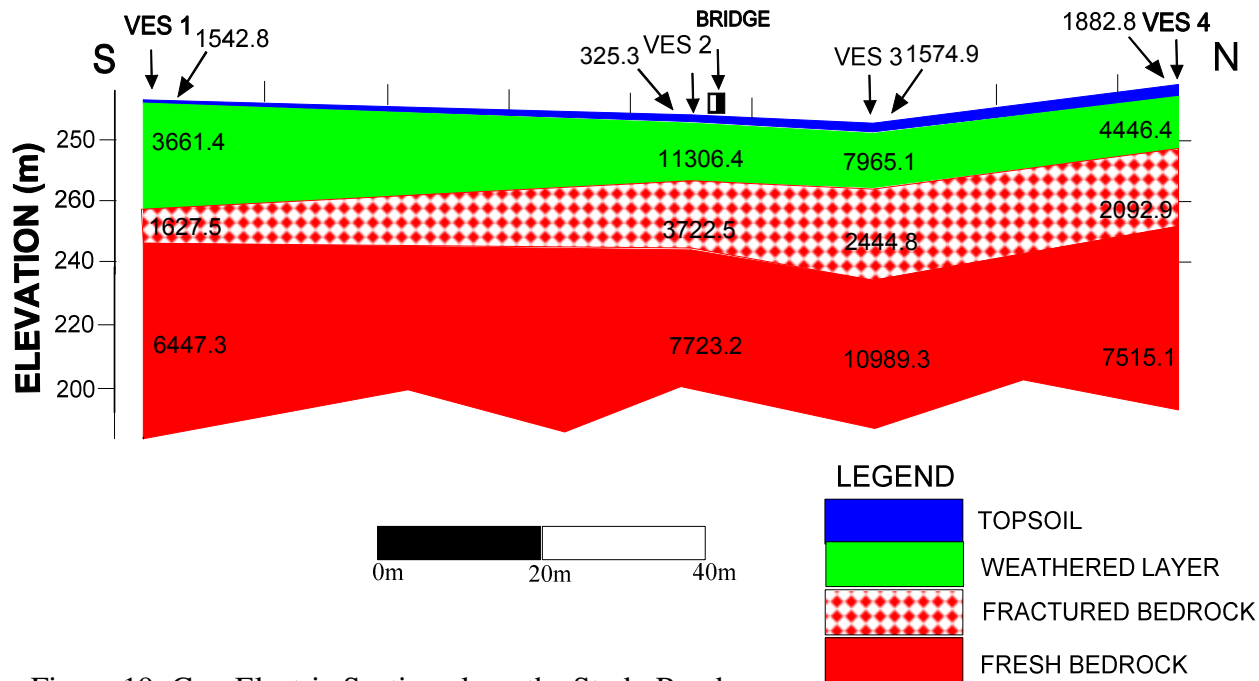


Figure 19: Geo-Electric Section along the Study Road.

The second layer is the weathered materials characterized by resistivity ranging from 3,661 to 11,306 Ohm-m. This resistivity range suggests a layer composed of coarse sand to rubble of quartzite rock. The thickness of this layer varies from 8.7 to 17.4 m. The third layer is the fractured zone characterized by resistivity ranging from 1,628 to 3,723 ohm-m. It was also observed that the cavity and depressed zones identified in the resistivity structures from the inversion of the CRPS data from the study area fall within this layer. On the basis of the relatively low resistivity that characterised the cavity and zones of depressions, the layer is presumed to consist of materials forming a cushion for the landslide that occurred in the past and creeping of soil materials from the hilly terrains. The thickness of this layer varies from 5.5 to 14.7 m.

The resistivity of the fresh bedrock varies from 10,989 to 6,447 ohm-m, indicating fresh bedrock. The depth to the fresh bedrock varies from 14.0 to 25.7 m. Since the topsoil is generally thin along the road segment, the weathered layer can effectively serve as sub-base and subgrade materials.

4.2 Results of the Geotechnical Tests

The results of the geotechnical tests conducted on the soil samples in the area are presented in Table 2 and discussed in the following sections.

4.2.1 Natural Moisture Content

The estimated values of the natural moisture content of the analysed soil samples are shown in Table 2. The natural moisture content gives information on the moisture condition of the soil. The natural moisture content of the soil sample ranges from 4 - 15%. This indicates that the entire soil samples have low to moderate moisture contents, which can be attributed to the low percentage of clay and implying that the soil samples are well drained.

4.2.2 Specific Gravity Test

As shown in Table 2, the specific gravity of the soil samples ranges from 2.64 to 2.66 g/cm³. Thus, by correlating the result of the soil test with typical values of specific gravities as recorded by (Bowels, 1992) in Table 3, it was observed that the soil samples are made principally of sand grains, which can be adjudged to be good as sub-base or subgrade materials due to their moderately high specific gravity values.

4.2.3 Grading Characteristics

The results of the grain size distribution analyses are also presented in Table 2 and Figures 20 - 23. Generally, the soil samples have percentage passing of the No 200 sieve (with 0.075 mm diameter) less than 35%, hence the soils range in group classification from A-1 to A-2 and are generally rated as excellent to good subgrade material based on the AASHTO 1962, Soil Classification System (Table 4).

Table 2 Summary of Geotechnical Results

Soil Sample Test	S1	S2	S3	S4
Natural moisture content (NMC)	4.3%	8.7%	11.2%	14.9%
Specific Gravity, g/cm ³	2.645	2.648	2.653	2.658
Particle Size Distribution (% finer 0.075mm)	1.6%	11.5%	13.5%	28.7%
Liquid Limit	19.1%	26.2%	27.3%	33.3%
Plastic Limit	1.6% (non-plastic)	22.2%	21.3%	22.4%

Linear Shrinkage	0.7	4.3	4.3	7.1
Plasticity index	Not applicable	4.0%	6.05%	10.95%
Permeability	1.98×10^{-3} cm/s	1.90×10^{-4} cm/s	1.35×10^{-4} cm/s	1.22×10^{-5} cm/s
Max Dry Density	1880 Kg/m ³	1840 Kg/m ³	1848 Kg/m ³	1810 Kg/m ³
Optimum Moisture Content	6.2%	5.0%	3.7%	4.6%
California Bearing ratio (CBR)	71%	66%	79%	31%
Unconfined Compression Strength, KPa.	Not applicable	218.9	244.7	312.0
Undrained shear strength, KPa.	Not applicable	102.4	122.4	156.0

Table 3: Specific Gravity Classification (After Bowels, 1992)

Type of soil	Specific Gravity,
Sand	2.65 – 2.67
Silty Clay	2.67 – 2.70
Inorganic clay	2.75 – 2.80
Soil with Mica	2.75 – 3.00

Table 4: Soil Classification System (AASHTO 1962)

	Granular Materials (35% or less passing No. 200)							Silt-Clay Materials (More than 35% passing No. 200)			
	Group A-1		Group A-3	Group A-2				Group A-4	Group A-5	Group A-6	Group A-7 (A-7-5, A-7-6)
	A-1-a	A-1-b		A-2-4	A-2-5	A-2-6**	A-2-7**				
Sieve Analysis Percent Passing											
No. 10	50 max	-	-	-	-	-	-	-	-	-	-
No. 40	30 max	50 max	51 min	35 max	35 max	35 max	35 max	36 min	36 min	36 min	36 min
No. 200	15 max	25 max	10 max								
Characteristics of fraction passing No. 40:											
Liquid limit	-	-	-	40 max	41 min	40 max	41 min	40 max	41 min	40 max	41 min
Plasticity index	6 max	N.P.		10 max	10 max	11 min	11 min	10 max	10 max	11 min	*11 min
Usual types of signi- ficant constituent materials	Stone Fragments gravel and sand		Fine sand	Silty or clayey gravel and sand				Silty Soils		Clayey soils	
General rating as subgrade.	Excellent to good							Fair to poor			

The analysed soil samples have percentage finer (percentage passing 0.075 mm sieve diameter) ranging from 1.6 - 28.7%. From the particle distribution curves, the soils can be classified as poorly graded soils. Poor grading might be attributed to the leaching of the soil residues from the hilly schistose quartzite ridges forming topsoil in the area. These soils are largely made up of coarse sand and are likely to serve as good geotechnical materials as subgrade or sub-base materials than elsewhere where the soils that are largely made of fines (silt and clay). However, according to Federal Ministry of Works and Housing (FMWH, 1972) specification as displayed in Table 5, the subsoil along the study road can be classified as suitable for subgrade, sub-base and base materials as their percentage by weight finer are generally less than 35%.

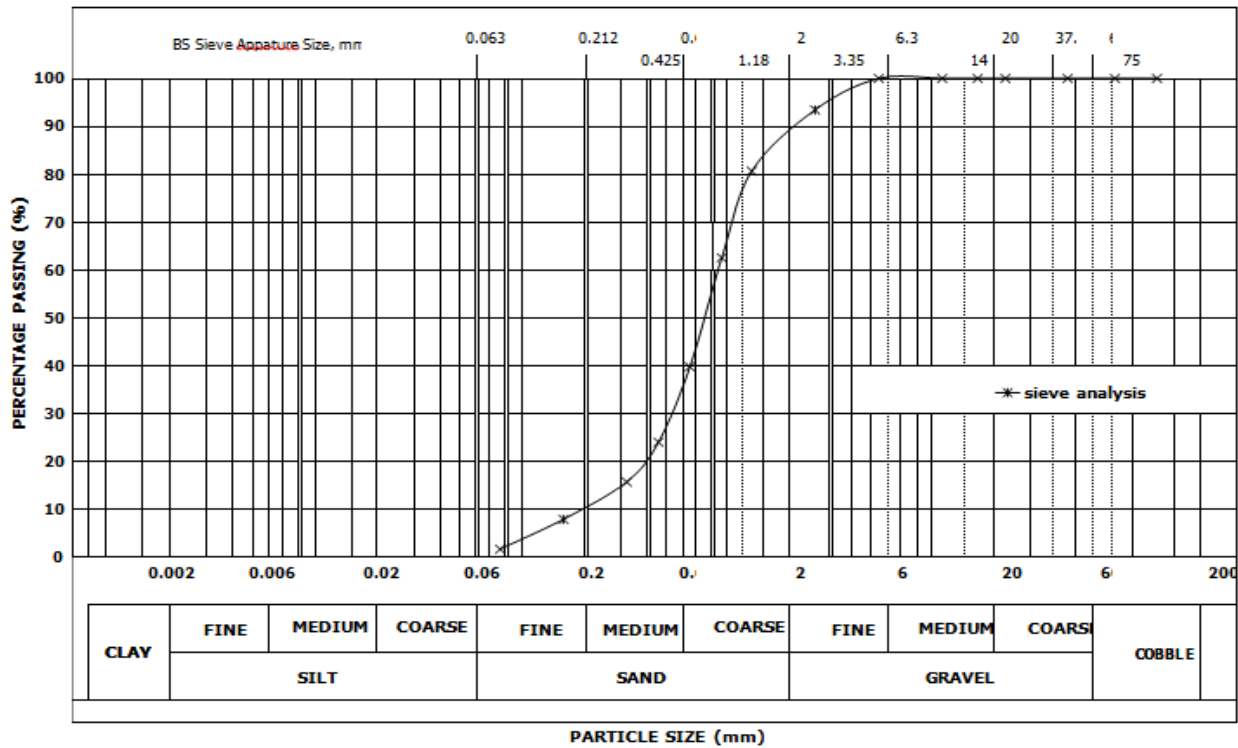


Figure 20: Particle Size Distribution Curve for Soil Sample S1

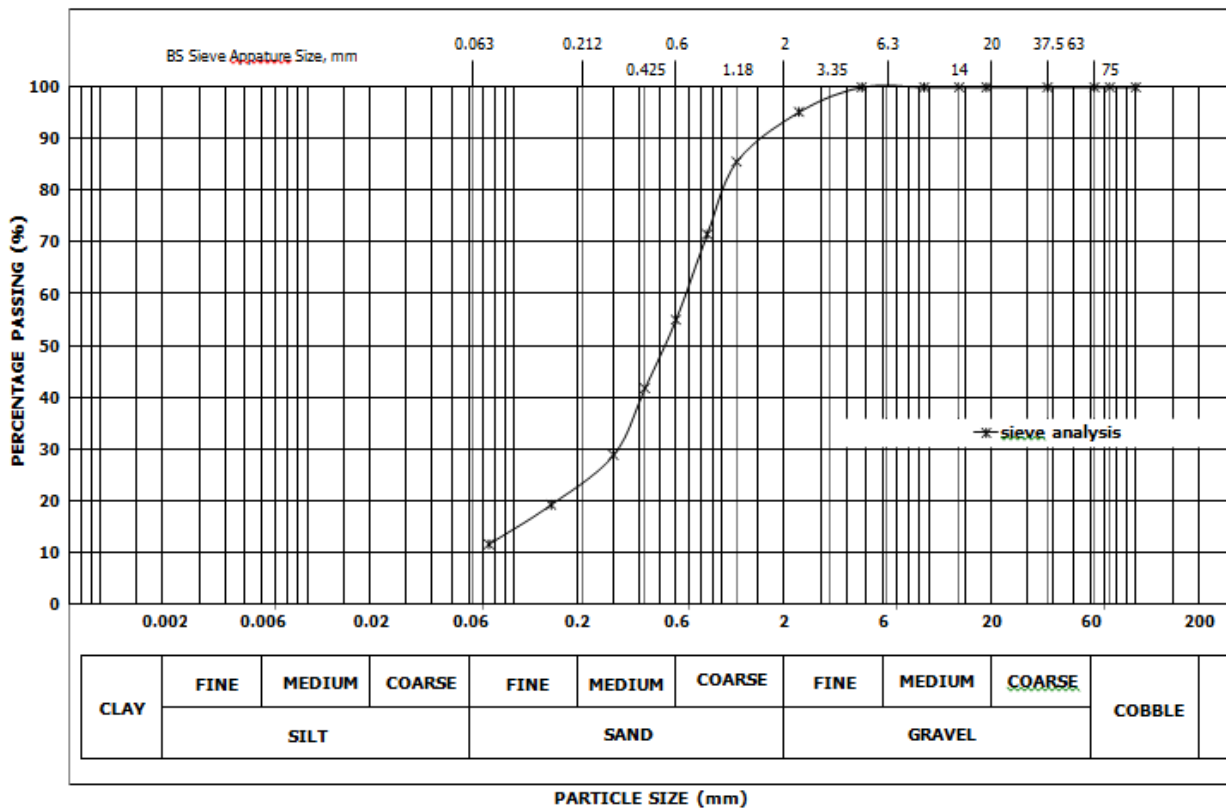


Figure 21: Particle Size Distribution Curve for Soil Sample S2

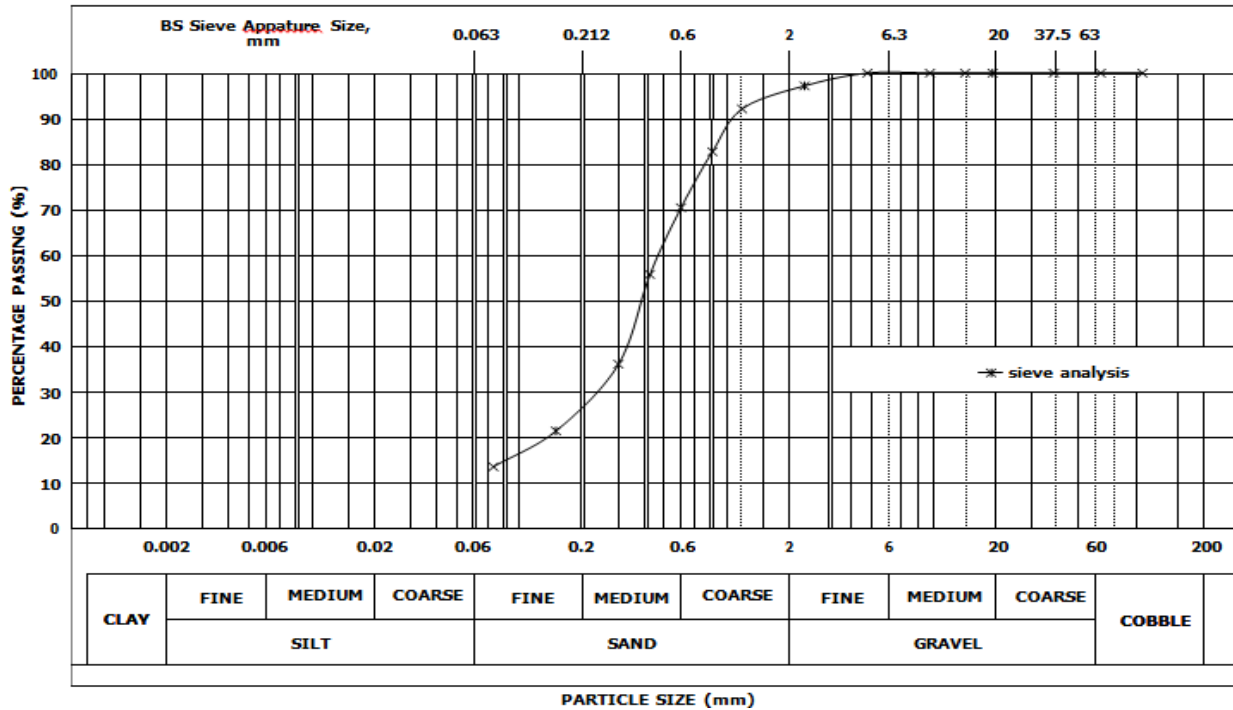


Figure 22: Particle Size Distribution Curve for Soil Sample S3

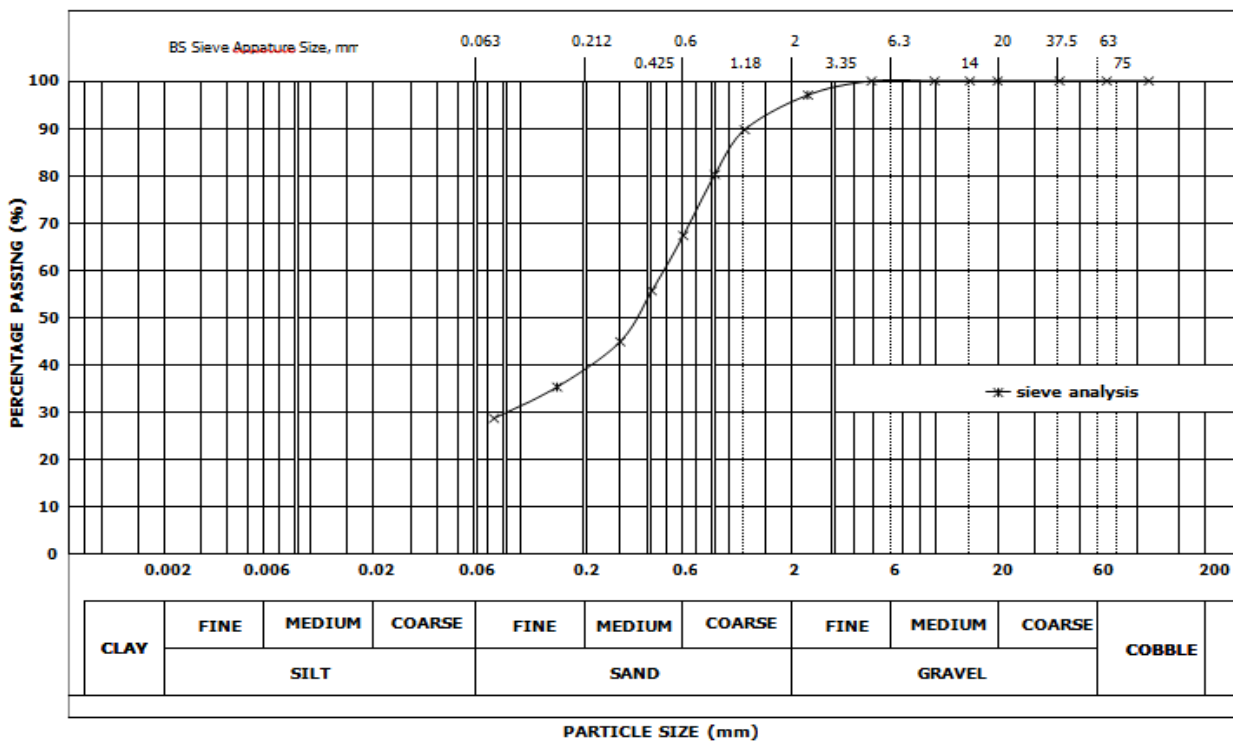


Figure 23: Particle Size Distribution Curve for Soil Sample S4

4.2.4 Consistency Limits

As shown in Table 2, the liquid limit of the soil samples ranges from 19 to 33%, while the plastic limit of the soil samples is in the range of 21 to 22%, with Sample S1 being non-plastic due to its low fine content (1.6%). Thus, the plasticity index of the soils sample ranges from 4 to 11%, with the Plasticity index of sample S1 being negligible (non-plastic). The federal ministry of works and housing (FMWH, 1972) recommends a liquid limit of 50% maximum, plastic limits of 30% maximum, and plasticity index of 20% maximum (Table 5) for subgrade materials for road construction.

In addition, from Table 2, the liquid limits of the soils beneath the study road are generally lower than 50%, while the plastic limits are lower than 30% and the plasticity index are lower than 20%. Hence, the soil samples in the study area fall within the (FMWH, 1972) specification, indicating that they are suitable for use as subgrade materials.

Table 5: Threshold Geotechnical Properties for Highway (Extracted from FMWH, 1972)

% Finer (0.075mm)	Liquid Limits (%)	Plastic Limits (%)	Plasticity Index (%)	Linear Shrinkage (%)	CBR (%)
≤ 35	50 maximums	30 maximums	20 maximums	8 maximums	80 minimum

Using the American Association of State Highway and Transportation officials (AASHTO) classification system shown in Table 4, the soil samples belong to group A-1 to A-2, hence the soil can be rated to be excellent to good sub-grade materials. The plasticity generally indicates low plasticity, which means the soils are expected to exhibit low swelling potential (Ola, 1982). According to (Brink *et al.*, 1992) this suggested that the soils in the study area with linear shrinkage below 8% would be inactive and in-expansive, thus suitable as a good sub-grade material.

4.2.5 Hydraulic Conductivity Test

The coefficient of permeability (K) obtained from the tested soil are presented in Table 2, with values ranging from 1.2×10^{-5} to 1.9×10^{-3} cm/s. From the permeability characteristics of soils, the coefficient of permeability of the soil tested can be generally rated as low to high permeability, which indicates that the soils obtained from the road segment are made of coarse sand materials, which can be adjudged to be good subgrade materials.

4.2.6 Compaction Characteristics

The Optimum Moisture Content (OMC) and Maximum Dry Density (MDD) obtained from the tested soils as presented in Table 2 ranges from 4 to 6% and 1,810-1,880 kg/m³ respectively for the soil samples. From the compaction tests carried out on the soil samples, the soils respective values of MDD at observed low OMC revealed that the soils are suitable materials for construction work along the road segment. As observed from Table 6, the MDD of the soil samples indicates that they fall within the fairly good subgrade materials.

Table 6: Foundation suitability of soils using range of Maximum Dry Density values (After Wood, 1937).

Max Dry Density kg/m ³	General Value as a subgrade foundation material
Over 2082.6	Excellent
1922.4 – 2082.6	Good
1762.2 – 1922.4	Fair
1602 – 1762.2	Poor
1121.4 – 1602	Very poor

4.2.7 California Bearing Ratio (CBR)

The California Bearing Ratio (CBR) values for the soil samples ranges from 31 to 79% as shown in Table 2, which fall short of the stipulated 80% minimum by the FMWH (1972) standards for subgrade soils (Table 5). On the basis of the (FMWH, 1972) standard, all the soil samples were found to have CBR value less than 80%, thus can be adjudged not suitable as subgrade materials. However, samples S1 and S3 with CBR values of 71% and 79% are closer to the minimum limit of 80%, they can be considered as fair subgrade material.

4.2.8 Unconfined Compression Test (UCS)

The results of the unconfined compression (UCS) test are also presented in Table 2. The soils have UCS value (q_u) ranging from 219 to 312 KPa. UCS test on sample S1 was not carried out because the soil sample was discovered to be non-plastic. Based on the general relationship between consistency and unconfined compression strength of soils proposed by (Das, 2000) and shown in Table 7, the soil

samples S2 – S4 can be classified as a very stiff soil that can allow the soils to be rated as good subgrade materials.

4.2.9 Undrained Shear Stress

The Mohr’s circle is a graphical means of determining the normal stress and shear stress on any plane in a 2D biaxial stress situation for the soil samples as shown in Figure 24 – 26. From the curves, the value at the peak of the circle was used in determining the undrained shear strength of the soil samples (undrained shear strength = $q_u/2$). The shear strength of the soil samples ranges from 102 to 156 KPa, which according to the classification system shown in Table8, the soils can be rated to be of high shear stress, indicating good subgrade materials.

Table 7: General Relationship of Consistency and Unconfined Compression Strength (After Das, 2000)

Consistency	Unconfined compressive Strength (KPa)
Very soft	0 -25
Soft	25– 50
Medium	50 – 100
Stiff	100 – 200
Very stiff	200– 400
Hard	>400

Table 8: Shear Strength Classification (BS EN ISO 14688 - 2:2004, 5.3)

Term based on measurement	Undrained Shear Strength Classification (KPa)
Extremely low	< 10
Very low	10– 20
Low	20 – 40
Medium	40 – 75
High	75 – 150
Very high	150 – 300

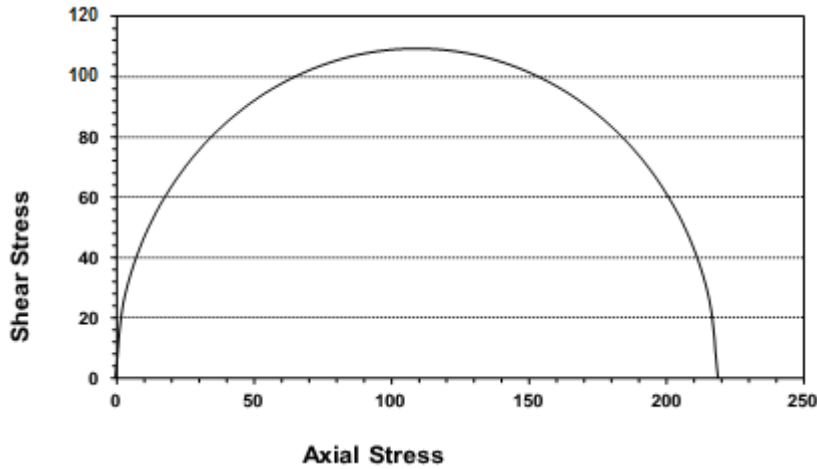


Figure 24: Mohr's Circle for Sample S2

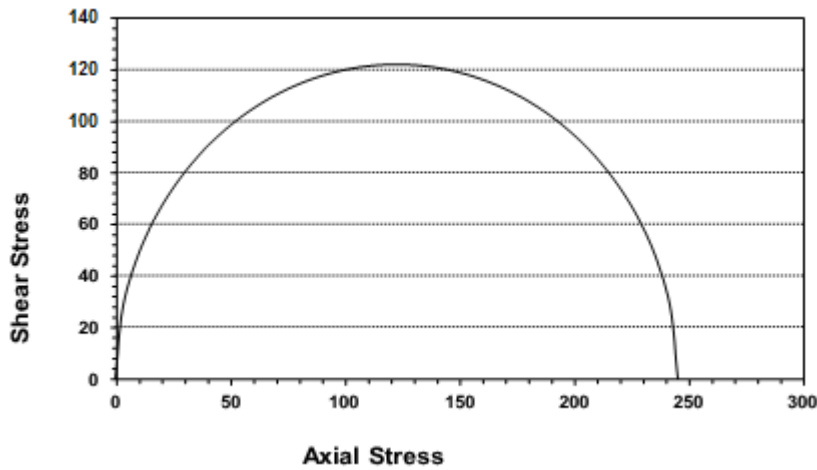


Figure 25: Mohr's Circle for Sample S3

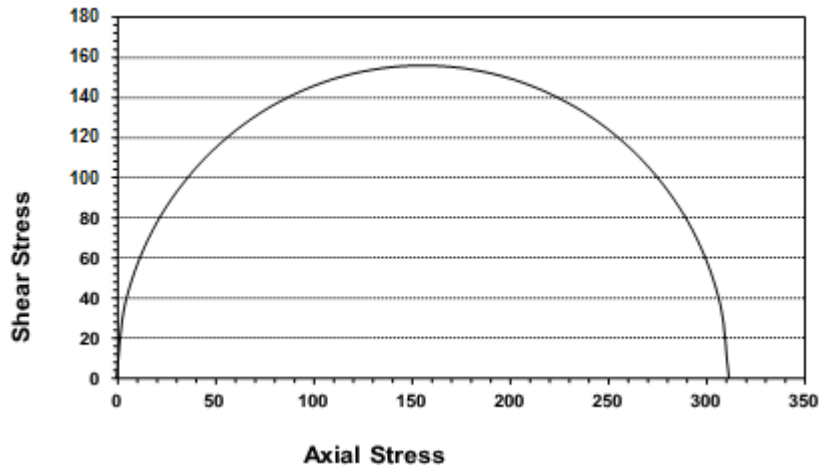


Figure 26: Mohr's Circle for Sample S4

5.0 CONCLUSION

In this paper, integration of geophysical method using the electrical resistivity method complemented with geotechnical investigations have been used to evaluate the engineering properties of the subsurface in a geomorphological unstable terrain of Oloruntele Town, a suburb of Oke-Igbo for the purpose of evaluating subsoil slope stability. The geophysical results show that the subsoil in the study area is characterized by high resistivity and a series of parallel fracture zones, which might have contributed to mass movement of rocks on the surface under gravitational force during a recent landslide that give birth to the river channel in the study area. The results from the resistivity data inversion revealed that though high resistivity values can be attributed to a competent subsoil condition where resistivity increases from the topsoil to the fresh basement layer, but the stability of the subsurface framework is greatly endangered by the negative impact of geologic features that occur as cavity, shear zones, fractured and faulted zone observed from the resistivity imaging using the HP/VES method. The VES interpretation show essentially Four geo-electrical layer, the topsoil, weathered layer, fractured bedrock and fresh bedrock. Topsoil layer resistivity range between $325\Omega\text{m}$ to $1,883\Omega\text{m}$ with thickness ranging from 0.8 to

1.6m. The weathered layer range in resistivity between 3,661 to 11,306 Ω m; this resistivity range suggests a layer composed of coarse sand to quartzite rock. The thickness of the layer varies from 8.7 to 17.4m, while the fractured bedrock resistivity ranges from 1,628 to 3,723 Ω m with a layer thickness of 5.5 to 14.7m. The fresh bedrock resistivity ranges from 6,447 to 10,989 Ω m. High resistivity values obtained for the topsoil and weathered layer indicate a competent subsoil condition, except in situations where geologic structures like fractures, faults or cavities could have reduced the competency of the layers. The geotechnical results generally show largely suitable geotechnical properties of the subsoil beneath the study area, the natural moisture content test indicates that the soil is well-drained, the specific gravity test indicated that the soils along the road segment contain high sand content. The particle size distribution test is indicative of textural characteristics and shows that the soil is composed of fine to coarse sand materials, which confirms high resistivity signature from the electrical resistivity method.

The linear shrinkage of the soils was lower than the maximum value of 8% recommended by (Madedor, 1983) for highway subgrade soils. The coefficient of permeability of the soil tested can be generally rated as low to high permeability, which indicates that the soils are made of a coarse sand material, which is a good subgrade material. The high Maximum Dry Density (MDD) of the soil samples indicates fairly good subgrade material. The California Bearing Ratio (CBR) of the soil sample falls below the recommended 80% minimum by (FMWH, 1972), but at two locations were observed to be between 71% and 79%. The Unconfined compressive strength and high undrained shear strength of the tested soil sample shows that it is very stiff soil indicating a good subgrade material.

It could be observed that the geotechnical results clearly revealed properties of materials that were not totally consistent and might not be uniquely derived except further approaches that were provided by the use of geophysical methods in this work are used to confirm or validate the findings. The geotechnical properties observed can be found to be impacted by lateral changes as well as depth-wise changes in

structures and facies of the subsoil materials. The soils in the area are found to be majorly sand and loose fragments of nearby quartzite ridge, which can easily move under gravity when heavy load are applied on them. It was therefore suggested that slope stabilization has to be carried out on the investigated section of the study area, while some sections in the study areamight not be able to carry very large axial loads due to the possible creeping of sandy materials characterizing the near surface geology that are geomorphologically unstable.

REFERENCES

- AASHTO (1962): ‘Road Test – Report 5 (Pavement Research)’’, Highway Research Board, Special Report 61E Washington D.C.
- Adeyemo, I.A., Omosuyi, G.O., 2012. Geophysical Investigation of Road Pavement Instability along part of Akure-Owo express way, Southwestern Nigeria. *Am. J.Sci. Ind. Res.* 3 (4), 191–197.
- Adiat, K.A.N., Adelusi, A.O., Ayuk, M.A., 2009. Relevance of geophysics in road failures investigation in a typical basement complex of southwestern Nigeria. *Pac. Jour. Sci. Tech.* 5 (1), 528–539.
- Adiat et al., 2017 K.A.N. Adiat, A.A. Akinlalu, A.A. Adegoroye Evaluation of road failure vulnerability section through integrated geophysical and geotechnical studies *NRIAG J. Astron. Geophys.*, 6 (2017), pp. 244-255, 2017.
- Ajayi, L.A., 1987. Thought on road failures in Nigeria. *Nigerian Eng.* 22 (1), 10–17.
- Akinlabi I. A., Akinrimisi O. E and Fabunmi M. A., 2018. Subsurface Investigation of Landslide Using Electrical Resistivity and Self-Potential Methods in Oke-Igbo, Southwestern Nigeria: Volume 6, Issue 5 Ver. I (Sep. – Oct. 2018), PP 67-74
- Alpin, L.M. (1966): The theory of dipole sounding in dipole methods for measuring earth conductivity: Consult Bureau, NY. Pp.1-60
- Bolaji, A.A. (2003). Highway Geotechnical Properties of Soils in some Sections of Ibadan-Ilorin Road, Nigeria, Unpublished B.Sc Dissertation Dept. of Civil Eng, Lautech Ogbomosho, Nigeria.
- Bowels, J.E. (1992). Engineering properties of soils and their Measurements, 4th International Edition. McGraw-Hill. Incorporations. pp. 53-58
- Brink, A. B. A., Parridge, J. C. and Williams, A. A. B (1992): Soil Survey for Engineering, Claredon, Oxford.
- British Standard B. S., (1990). Methods of testing of soils for civil engineering purposes. British Standard Institution.
- British Standard B. S., (2004). Methods of testing of soils for civil engineering purposes. British Standard Institution.

- Das, B. M. (2000). Fundamentals of geotechnical engineering. Pacific Grove, CA: Brooks/Cole. p. 593.
- Federal Ministry of Works and Housing (1972). Highway Manual Part 1 Road Design, Federal Ministry of Works and Housing, Lagos.
- Folami, S. L., (1998). Aeromagnetic anomalies over the amphibolite complex in itagumodi area, southwest, Nigeria journal of Mining and Geology 27, (1): 31-34
- Hubbard, F.H. (1975). Precambrian Crustal development in Western Nigeria: Indication from Iwo Region. Geological society of America Bulletin, Vol. 86, pp. 548-554
- Ikubuwaje, C (2008). Geotechnical Characterization of Erosion Activities in A Built-Up Environment: A Case Study of Okeigbo, South-western Nigeria. An Unpublished M.Sc Thesis. Pp 21 – 39
- Ikubuwaje, C, Obasi, R. A, and Jegede, G. (2013). The Geomorphologic Denudation of Oke-Igbo area of Ondo State, Southwest Nigeria: A Hydro-Climatic Influence. Volume 3, Issue 5 (Mar.- Apr. 2013), pp. 62-67.
- Jegede, G. (1999). The effect of Groundwater and Soil properties on High pavement failure at Ayewa Locality the journal of Techno science Vol.3, pp. 41-43.
- Madedor, A.C. (1983). Pavement design guidelines and practice for different geological area in Nigeria. In: Ola SA (Ed) tropical soil of Nigeria in engineering practice. A.A Balkema, Rotterdam, pp. 291-297.
- Mesida, E.A., 1987. The relationship between the geology and the lateritic engineering soils in the northern environs of Akure, Nigeria. Bull. Int. Assoc.Eng. Geol. 35, 65–69.
- Momoh, L.O., Akintorinwa, O., Olorunfemi, M.O., 2008. Geophysical investigation of highway failure – a case study from the basement complex terrain of southwestern Nigeria. J. Appl. Sci. Res. 4 (6), 637–648.
- Ola, A. (1982). Geotechnical properties of an attapulgitic clay shale in north western Nigeria. Eng. Geol. 19: 1-13
- Olayanju, G .M, Mogaji K.A, Lim H. S. and Ojo T. S (2017). Foundation integrity assessment using integrated geophysical and geotechnical techniques: case study in crystalline basement complex, southwestern Nigeria. J. Geophys. Eng.14 (2017) 675–690 (16pp)
- Oladapo, M.I., Olorunfemi, M.O., Ojo, J.S., 2008. Geophysical investigation of road failures in the basement complex areas of southwestern Nigeria. Res. J. Appl. 3(2), 103–112.
- Olorunfemi, M.O, Ojo J.S., Olayinka A.I. and Mohammed M.Z. (2000). “Geophysical investigation of suspected spring in Ajegunleigoba, near Akure, southwestern Nigeria” Global journal of pure and applied sciences, Vol.7, No 2: pp 311-320
- Olorunfemi, M.O, A.I. Idoringe, H.O. Fagunloye and O.A ogun (2004). Assesment of Anomalous seepage condition in the opa Embankment, Ile-Ife, SouthweestteernNigeria. Global journa of Geological science Vol.2, No.2:191-198.
- Rahaman, M.A. (1988). Recent advances in the study of the Basement Complex of Nigeria. In: Oluyide, P.O., Mbonu, W.C., Ogezi, A.E., Egbuniwe, I.G., Ajibade, A.C. and Umeji, A.C. (eds.). *Precambrian Geology of Nigeria*, G.S.N., pp. 11 – 41
- Rahaman, A.A. and Malomo, S. (1983). Sedimentary and crystalline rocks of Nigeria. Precambrian Geology of Nigeria. Geological Survey of Nigeria. Pp. 11 - 44

Vander Velper, B.P.A. (1988). Resist version 1.0, Msc. Research project, ITCC, Delf Netherland.

Woods, K.B. Compaction of Embankments. Proceedings of Highways Resources, Washington
18(2): 142-181, 1937.